NOTICE: This Material May Be Protected By Copyright Law (Title 17 U.S. Code)

3
Nanotubes, Nanowires, and Nanocantilevers in Biosensor Development

Jun Wang, Guodong Liu, and Yuehe Lin

3.1
Introduction

Recent developments in designing and synthesizing conducting one-dimensional (1D) nanostructured materials, including carbon nanotubes (CNTs) and nanowires, etc., have attracted much attention across scientific and engineering disciplines because of their great potential for replacing conventional bulk materials in micro- and nanoelectronic devices [1, 2] and in chemical [3, 4] and biological sensors [4–9]. Various methodologies and technologies have been developed to fabricate 1D conducting nanomaterials [10, 11]. For example, chemical methods, including catalytic vapor deposition (CVD) have been widely used to synthesize CNTs [12, 13] and silicon nanowires [14, 15] on catalytically patterned substrates at desired sites with controlled orientations. Microfabrication [10, 11], soft lithography techniques [10, 11], and electric fields [16], etc. have been employed to fabricate highly oriented 1D nanomaterials. Various electrochemical techniques have been developed to fabricate 1D conducting polymer nanowires [17, 18]. New techniques are being explored to synthesize new 1D nanomaterials.

One-dimensional nanostructured materials as building blocks for biosensors are promising because of their unique electronic, optical, chemical, and mechanical properties, which are intrinsically associated with their low dimensionality and the quantum confinement effect. Therefore, 1D nanomaterials have broad applications in developing various types of biosensors, e.g., electrical [19, 20], optical [21], and mechanical [22] (nanocantilever biosensors). For example, CNTs exhibit excellent electronic properties. They can be used as molecular wires for facilitating electron transfer on the surface [23]. One-dimensional nanomaterials have a high aspect ratio, which makes them exhibit extreme sensitivity and superior response. Owning to their high sensitivity, 1D nanomaterials can be used to construct label-free biosensors. This will be very attractive and avoid exhausting and complicated labeling. With the ever-decreasing sizes of these 1D nanostructures, the "bottom-up" chemical approach is playing an increasingly important role because of its capability to make much smaller features compared to the "top-down" approach. So, combined with bottom-up techniques, 1D nanomaterials are ideal building blocks for

Nanotechnologies for the Life Sciences Vol. 8
Nanomaterials for Biosensors. Edited by Challa S. S. R. Kumar
Copyright © 2007 WILEY-VCH Verlag GmbH & Co. KGaA, Weinheim
ISBN: 978-3-527-31388-4

constructing miniature biochips. The detection mechanism with these tiny nanosensors is based on chemical interactions between the surface atoms of 1D nanostructured materials and adsorbed molecules. This interaction will provide a direct electronic readout within a few seconds of electron-donating or -withdrawing molecules adsorbing onto the nanomaterials. A miniature biochip based on 1D nanomaterials will be implanted in the body and will detect multiple biological molecules *in vivo*! In general, these 1D nanomaterials are expected to play an important role in the development of various emerging technologies that will improve the way we live.

Biosensors based on 1D nanomaterials have shown great advantages. However, real applications in biological diagnosis are a long way off. A major challenge remains to fully exploit the 1D nanostructure with one lateral dimension between 1 and 100 nm. For example, 1D nanostructured material-based biosensors need to bind biological recognition molecules onto the device. It is a great challenge to individually address high-density biomolecule nanoarrays. There is also a need for deconvolution of noise from the signals. To analyze proteomic signatures, a major challenge will be to identify signatures from low-concentration molecular species in the presence of an extremely high concentration of non-specific proteins.

As a branch of nanotechnology, 1D nanomaterial-based biosensor development has made great progress. Each year, thousands of articles on nano-related biosensors are published, and many reviews have appeared in different journals [24, 25]. The present chapter introduces reviews on biosensor development based on 1D nanomaterials, CNTs, semiconducting nanowires, and some cantilevers. The chapter is comprehensive – previous reviews on nanomaterials-based biosensor development have focused on one of 1D nanomaterials, e.g., either carbon nanotubes or nanowires. The emphasis here, however, is on CNTs and electrochemical/electronic biosensor developments. Section 3.2 gives a detailed description of carbon nanotubes-based biosensor development, from fabrication of carbon nanotubes, the strategies for construction of carbon nanotube based biosensors to their bioapplications. In the section on the applications of CNTs based biosensors, various detection principles, e.g., electrochemical, electronic, and optical method, and their applications are reviewed in detail. Section 3.3 introduces the method for synthesis of semiconducting nanowires, e.g., silicon nanowires, conducting polymer nanowires and metal oxide nanowires and their applications in DNA and proteins sensing. Section 3.4 simply describes the development for nanocantilever-based biosensors and their application in DNA and protein diagnosis. Each section starts with a brief introduction and then goes into details. Finally, Section 3.5 summarizes the development of 1D nanomaterials based biosensors.

3.2
Carbon Nanotubes in Biosensor Development

CNTs, rolled graphene sheets, were discovered in 1991 by Iijima [26] following the historical finding of the new fascinating member of the carbon family –

"Buckyball" fullerene (carbon nanocage) and other nanocarbon particles [27]. CNTs have basic sp^2 carbon units that comprise a seamless structure with hexagonal honeycomb lattices, being several nanometers in diameter and up to hundreds of microns long. CNTs can be divided into two major groups, i.e., single-wall CNTs (SWCNTs) and multiwall CNTs (MWCNTs). SWCNTs represent a single graphite sheet rolled flawlessly, demonstrating a tube diameter of 1 to 2 nm, whereas MWCNTs show concentric and closed graphite tubules with diameters ranging from 2 to 50 nm and an interlayer distance approximately 0.34 nm [28]. Typical SWCNTs have an open-ended nanostraw or a capped nanohorn tubular structure. Because of the highly oriented architectures, these novel nanostructures exhibit physicochemical properties different from those of bulk graphite and diamond and thus provide their unique electronic, chemical, thermal, and mechanical properties [29, 30]. Since the early 1990s, CNT science has been one of the fastest growing areas of research in chemistry, physics, materials, and life technologies. The important properties and possible potential applications of CNTs have been reviewed recently [31–35].

The first type of CNT-based sensor was prepared by using MWCNTs mixed with bromoform as a binder packed into a glass capillary. This modified electrode exhibited remarkable improvement with regard to the electrochemical oxidation of dopamine [36]. Since then, work has concentrated on their electrocatalytic performance towards the redox behaviors of biomolecules [37, 38], especially towards the fabrication of effective, prototype deoxyribonucleic acid (DNA) and glucose biosensors [39, 40]. Recent summaries of the preparation conditions, interferences, interfacing, comparison, or analytical promise of the CNT-based sensors can be found in more specific reviews [41–43].

3.2.1 Preparation and Purification of CNTs

CNTs synthesis has mainly involved three major methods: the carbon arc-discharge method, or electric arc discharge (EAD) [26, 44], the laser vaporization of a graphite electrode or laser ablation (LA) [45], and a chemical method, CVD [11, 12]. EAD uses a direct current arc between carbon electrodes within a noble gas, like argon or helium [26]. In CVD, the CNTs are formed by the decomposition of the gaseous hydrocarbon at 700–900 °C and atmospheric pressure [46]. Materials produced by the EAD and LA protocols are in the forms of porous membranes and powders that require further processing. CNTs can be grown directly on substrates by the CVD process. Among these three techniques, the CVD is the most promising synthesis route for economically producing large quantities of CNTs. This is because the catalyst-involved CVD can use a lower temperature to form CNTs than the other two techniques. In addition, the catalyst can be deposited on a substrate, which allows for ordered synthesis and the formation of novel structures. CNT-based research for sensor applications only gained momentum after these highly oriented, large-scale productions emerged.

MWCNTs were first made by Yacaman et al. [47] followed by others [12, 13, 45]. Their experimental set-up usually consists of a high-temperature oven in which the catalysts are placed onto a highly resistant ceramic or metal plate. The nature and yield of the deposit obtained in the reaction are controlled by varying different parameters, such as the nature of the metals and the supports, the hydrocarbon sources, the gas flows, the reaction temperature, and the reaction time. By selecting the proper conditions, both the physical (e.g., length, shape, diameter) and chemical (e.g., number of defects, graphitization) properties of MWCNTs can be designed in advance. The choice of catalysts is vital in growing a good quality of CNTs and has been a subject for several research groups. Supported Co, Ni, and Fe catalysts were found to be the most active in the CVD growth thus far, although the metals and supports demand different temperature ranges [48, 49].

The first SWCNTs were reported by Iijima and Ichihashi when employing the EAD set-up with a low product yield [50]. This synthesis was significantly improved in 1996 when Dai et al. demonstrated that LA can be an effective way to grow highly uniform tubes that have a greater tendency to form aligned bundles than those prepared using EAD [45]. These ordered CNTs were fabricated by laser vaporization of a carbon target in a furnace at 1100 to 1200 °C, which was a much lower temperature than that was previously thought necessary for nanotube formation. A Co-Ni catalyst assists the growth of the nanotubes, presumably because it prevents the ends form being "capped" during synthesis. In a later work, the same group showed that high quality SWCNTs could be produced by CVD decomposition of methane on supported transition metal oxide catalysts [51]. The experimental set-up was similar to apparatus generally producing multiwalled nanotubes; however, some factors, including the catalyst composition, the support, and the hydrocarbon, were different. Fe_2O_3 was found to be significantly more efficient in SWCNT production than CoO or NiO. Methane was used instead of the generally applied acetylene or ethylene because of its kinetic stability at high temperatures. Since there is no pyrolytic decomposition, the carbon atoms needed for the growth of nanotubes are produced by a catalytic reaction from the methane on the metal surfaces. The reaction time was dramatically reduced from the usually applied hour(s) to 10 min, and thus it prevents the outer surface of the nanotubes from being coated with amorphous carbon. In the following year, Colomer et al. proved, after viewing the nanotube bundles by transmission electron microscopy, that the best yield of SWCNTs is obtained by using a Fe-Co binary mixture supported by alumina [52]. Other groups have explored the possibility of extending their successful approach for MWCNTs into SWCNTs growth, mainly focusing on CVD [12, 13, 46–49].

High-purity CNTs can be, theoretically, achieved by optimizing the synthetic routes, and this should be viewed as part of the overall performance of the proposed preparation protocol. Nevertheless, the as-synthesized CNT materials unavoidably contain significant amounts of impurities, including amorphous carbon, graphite particles, and metal catalysts. The purification schemes that have been developed usually take advantage of differences in the aspect ratio [53] and oxidation

rate [54] between the nanotubes and the impurities. Zhou et al. proposed a method that can reach final product purity over 95% [55]. The protocol combines hydrogen peroxide reflux with filtration that can effectively remove most of the impurities. Recently, Chiang et al. modified a gas-phase purification technique previously reported by Smalley and others [53] that uses a combination of high-temperature oxidations and repeated extractions with hydrochloric acid. This improved procedure significantly reduces the amount of impurities (catalyst and non-nanotube forms of carbon) within the nanotubes, increasing their stability remarkably. The onset of decomposition of the purified nanotubes (determined by thermal gravimetric analysis in air) is more than 300 °C higher than that of the crude nanotubes. Transmission electron microscopy analysis of the purified nanotubes reveals near complete removal of iron catalyst particles. The iron content of the nanotubes was reduced from 22.7 wt.% in the crude nanotubes to less than 0.02 wt.% in the final product. Nanotubes purified by this method can be readily dispersed in common organic solvents, in particular *N,N*-dimethylformamide, using prolonged ultrasonic treatment. These dispersions can then be used to incorporate single-wall CNTs into polymer films.

3.2.2 Construction of CNT-based Biosensors

Interest in exploring CNTs in biosensor fabrication has grown exponentially since the inception of CNTs in 1991 [26] and the first CNT-based sensor report [36]. Following the preparation and purification of a large quantity of CNTs as discussed above, the immobilization of these sensing layers onto the transducer support is introduced below. Basically, these CNT immobilizations have been based on dispersion, solubilization, adsorption, functionalization, composite entrapment, and other surface anchoring protocols.

3.2.2.1 Dispersion and Stabilization by Oxidative Acids

The well-ordered, all-carbon hollow CNTs possess unique walls and ends and thus resemble the sensing properties of basal planes of pyrolytic graphite (through their walls) and of edge planes of pyrolytic graphite (through their open ends). This sensing mechanism, in addition to their high surface-to-volume ratio, high chemical and thermal stability, high tensile strength, and elastic nanostructures, has made them excellent candidates for sensor fabrication. However, the spontaneous coagulation and the lack of solubility of CNTs in aqueous media is a major challenge for their application. To prevent coagulation of the as-synthesized CNTs, oxidative acid treatments are usually explored, including refluxing and sonication in a concentrated mixture containing sulfuric acid and nitric acid, as reported by Smalley's group [56]. This procedure, while occasionally generating surface defects and tube shortening, can produce abundant carboxylated sites on the CNT walls and caps. A dark stable aqueous suspension of CNTs can be achieved after removing access acids. More recently, Mallouk's group have reported that a stable SWCNT aqueous dispersion at concentrations above 0.3% can be obtained as a re-

sult of the hydrogel formation. This follows the treatments by a mixture containing $H_2SO_4 + (NH_4)_2S_2O_8 + P_2O_5$ and a subsequent mixture with $H_2SO_4 + KMnO_4$ [57]. Similar approaches have also been reported for a stable aqueous MWCNT hydrogel formation [58].

3.2.2.2 Dispersion by Surfactant Interaction

To preserve the intact CNT nanostructures after dispersion, a noncovalent stabilization/immobilization might be attractive. Simple physical stabilization, such as centrifugation, filtration, distillation, and sonication, in coupling with simple immobilization, including evaporation, casting, or spin coating, can be directly applied for respective sensor fabrications [35, 36]. Nevertheless, the hydrophobicity of the CNT walls, which accounts for vast majority of the tubes, is a major barrier when it comes to dispersing and manipulating the sensor surface and anchoring in a controlled manner.

Considering the relatively hydrophilic caps of CNTs, the noncovalent surfactant- and polymer-assisted aqueous dispersion may offer an alternative to overcome the drawbacks of the simple physical stabilization [59, 60]. The systematic study of the SWCNT dispersion in various surfactants has been reported and tabulated by Sun et al. [41], with the CNT solubilities ranging 10–50 mg mL^{-1}.

3.2.2.3 Polymer-assisted Solubilization

Because of the pseudo-amphiphilic feature of CNTs, due to their hydrophilic carboxylated ends and hydrophobic sidewalls, various ionic and nonionic polymers, such as poly(*p*-phenylenevinylene) [59], poly{(m-phenylenevinylene)-*co*-[2,5-dioctyloxy-(*p*-phenylene)-vinylene]}, [60] or poly(ethylene oxide)-poly(propylene oxide)-poly(ethylene oxide) triblock polymers, have been reported to "wrap" CNT in polymeric chains to facilitate dispersing and to stabilize the nanotubes, without impairing their physical properties [59, 60]. Wang et al. developed a method that directly applied Nafion polymer-assisted CNT dispersion in sensor fabrication [61]. Similar to other polymers used to wrap and solubilize CNTs, Nafion bears a polar side chain and can produce a CNT suspension in phosphate buffer or alcohol solution. Increasing the Nafion content from 0.1 to 5 weight percent (wt.%) results in dramatic enhancement of the solubility of both single-wall and multiwall CNTs (Fig. 3.1). A homogeneous solution of the Nafion/CNT complex is observed in Nafion solution, but no such solubilization is observed in ethanol or phosphate-buffer solutions containing no Nafion. The CNT/Nafion association does not impair the electrocatalytic properties of CNTs with respect to the redox reaction of hydrogen peroxide. The Nafion-induced solubilization of CNT thus permits various applications, including the modification of electrode surfaces for preparing amperometric biosensors, and field-effect transistors [62].

3.2.2.4 CNT Adsorption on the Transducer Substrate

Although the dispersion and distribution of CNTs in aqueous media have proved to be challenging, some non-polar organic solvents such as *N*,*N*-dimethylformamide (DMF) cause less coagulation of the tubes and thus permit a greater extent of dis-

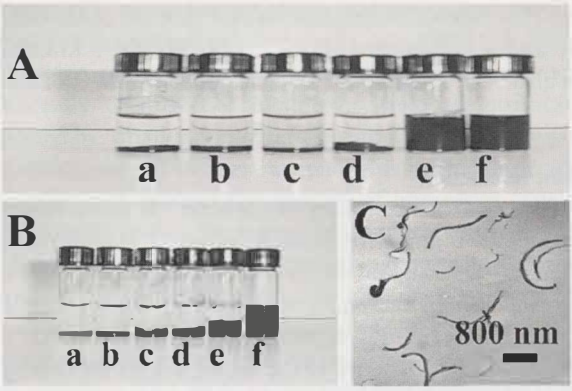

Fig. 3.1. Photographs of vials containing 0.5 mg mL^{-1} SWCNT (A) and MWCNT (B) in different solutions: phosphate buffer (0.05 M, pH 7.4) (a), 98% ethanol (b), 10% ethanol in phosphate buffer (c), 0.1% Nafion in phosphate buffer (d), 0.5% Nafion in phosphate buffer (e), and 5% Nafion in ethanol (f). (C) TEM image of a 0.5% Nafion solution containing MWCNT (0.3 mg mL^{-1}). (Reprinted with permission from Ref. [61]. © 2003 American Chemical Society.)

persion. This organic solubility offers the possibility for directly coating or spin casting of the CNT organic solution onto the sensor substrate and subsequent solvent evaporation. Re-immersion of these resultant CNT-based sensors into aqueous media showed no loss of operational performance and thus provides proof of strong adsorption on the surface. The first CNT-based sensor by Britto and co-authors was based on nanotubes solubilized in bromoform as a binder material following packing into a glass tube to complete the sensor construction [36]. Presently, many sensors still use this approach because of the ease of fabrication. The most often used substrates are glassy carbon, gold, platinum, carbon fiber, and glass. Lately, a protocol derived to co-incorporate some recognition reagent has been reported [63, 64]. Although these protocols are almost the simplest and most convenient ways to fabricate CNT-based sensors, the non-specific CNT adsorption needs to be addressed to gain greater control over their random distribution if a highly reproducible and stable sensor is demanded.

3.2.2.5 Surface Functionalization of CNTs

Biosensors need specific surface recognition towards targets, and have thus promoted the modification of CNTs. These modifications usually start with the CNTs' sidewalls, ends, and defects, which are rich in nanotube-bound carboxylic groups. The latter are the nondestructive outcome of oxidative acid pretreatment on CNTs. The external-added functional molecules can be as small as simple amino acids or as large as protein macromolecules. Linkages between the nanotubes and the functional components, with or without coupling agents, are based on carboxylate chemistry via amidation and esterification, as well as ionic interaction schemes.

Accordingly, these functionalizations can be covalent or noncovalent bonding in nature.

Liu et al. have used dicyclohexylcarbodiimide (DCC), a coupling reagent which converts the carboxylate ends of the SWCNTs into carbodiimide leaving groups, to react with amines on cysteamine ($NH_2CH_2CH_2SH$) [65]. The single-walled nanotubes with free thiol terminal groups then covalently attached onto substrate gold surface through a self-assembly process. Although atomic force microscopy (AFM) and transmission electron microscopy (TEM) have revealed different surface morphology of the resultant modified surfaces [66], this functionalization protocol offers control over the spatial distribution, lengths, and other surface patterns of the nanotubes aligned on the substrate by adjusting the assembled amount and time. Gooding and coauthors employed a similar carbodiimide-activated conjugating method in immobilization of microperoxidase (MP-11) onto the perpendicularly aligned nanotubes that were pre-anchored on the cysteamine-modified gold electrode [66]. Other direct bonding or electrostatic complexing approaches include using such as bridging metal ions to connect a polyelectrolyte-modified surface and the carboxylic acid terminated tubes [67] and complexing with an oppositely charged polyelectrolyte [66]. While these approaches provide various patterned nanotubes, a major concern lies in that the aligned tubes have little support and, therefore, the electrodes may lack robustness [67].

To elucidate the covalent, electrostatic, and nonspecific contributions to protein–SWCNT interaction, Davis et al. carried out the experiments of amidation both in the presence and absence of the coupling reagent DCC [69, 70]. They discovered that glucose oxidase is adsorbed along the length of CNTs randomly distributed on a glassy carbon electrode. Though coupling can be controlled, to a degree, through variation of tube oxidative pre-activation chemistry, careful control experiments and observations made by AFM suggest that immobilization is strong, physical, and does not require covalent bonding. Figures 3.2 and 3.3(a) exhibit their proposed protein–nanotube conjugates, which were readily characterized at the molecular level by AFM. Ferrocene monocarboxylic acid behaves as a mediator to promote charge transfer communication between electrode surface and the enzyme molecules. Under such conditions, the glucose signal was 10× greater than if only glucose oxidase was adsorbed onto the glassy carbon electrode without CNTs (Fig. 3.3b). This approach demonstrated the possible device application; protein attachment appears to occur with retention of the native biological structure. The role of nanotubes in this proposed glucose sensor was to provide (1) the high-aspect ratio electrode to which high capacity glucose oxidase loading was achieved, and thus greater signals were generated from more active enzyme interfacing and (2) provide possible direct electrical communication between a redox-active biomolecule and the delocalized π system of its CNT support [71].

3.2.2.6 Composite Entrapment and CNTs Bulky Electrode Material

The first nanotube composites were prepared by Ajayan and coauthors by mechanically mixing MWCNTs and epoxy resin [72]. Because CNTs themselves could be

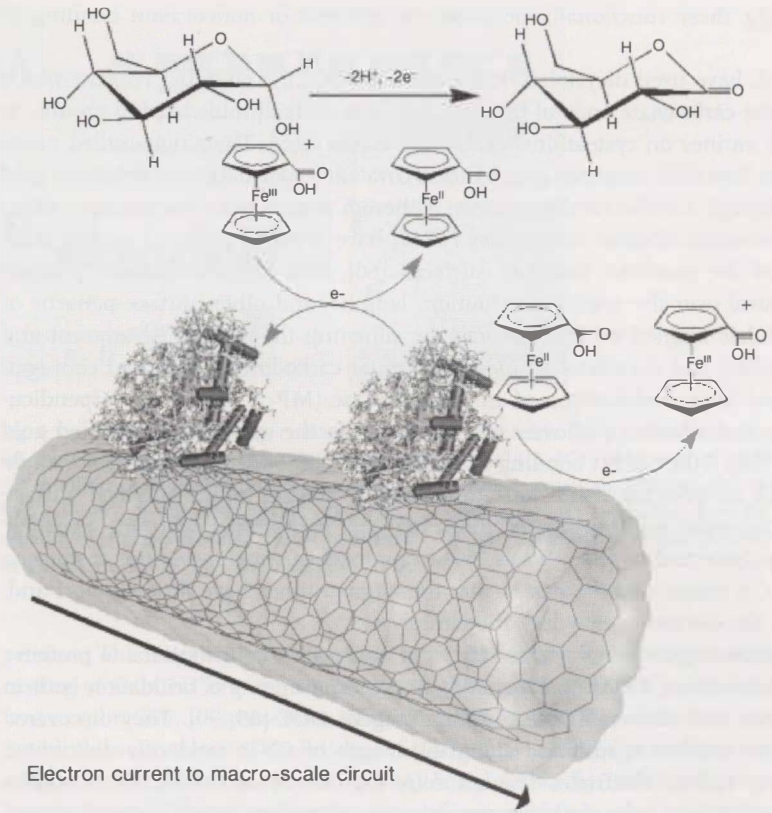

Fig. 3.2. Schematic representation of the "SWCNT Glucose Biosensor." Solution-phase D-glucopyranose is turned over by oxidase enzymes immobilized on the nanotubes. This redox process at the enzyme flavin moieties is "communicated" to the nanotube π system through the diffusive mediator ferrocene monocarboxylic acid. The redox action of the ferrocenes at the nanotube surface ultimately generates a quantifiable catalytic current that is characteristic of substrate detection and turnover. (Reprinted with permission from Ref. [70]. © 2003 Wiley-VCH.)

viewed as an extreme form of conducting polymer, the combination of nanotubes with conventional π-conjugated conducting polymers offers new electronic properties and high surface area capacity. This well suits the integration of substrate and transducer when making biosensors.

Wallace et al. combined MWCNTs and glucose oxidase to be embedded into polypyrrole (Ppy) with 0.1 M $NaClO_4$ as supporting electrolyte [73]. Such an enzyme electrode retains its stability at 70% after 3 days storage in the dry state at 4 °C. The use of these 3D electrodes offers advantages in that large accessible enzyme loadings can be obtained within an ultrathin layer. The iron-loaded nanotube tips (generated from CNT preparation) also contribute partial catalytic capacity toward H_2O_2 oxidation. A biosensor based on Ppy/DNA composite covered CNT under-

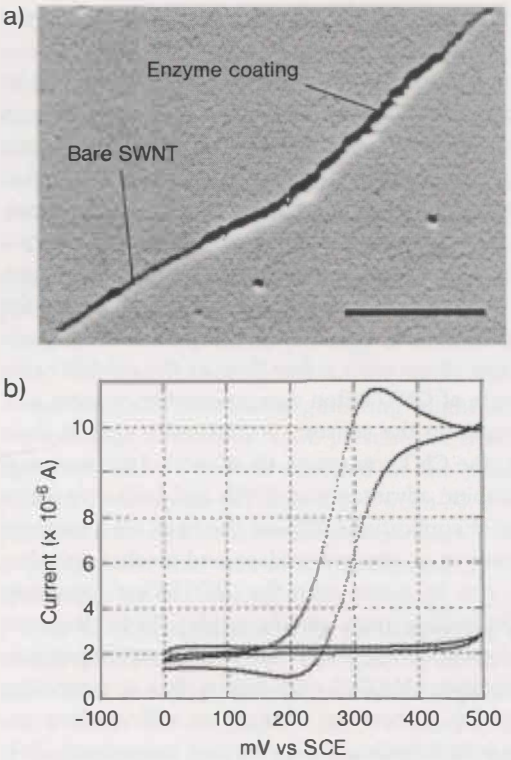

Fig. 3.3. (a) TMAFM amplitude micrograph of a GOX-modified SWCNT in which a high degree of enzyme loading is apparent. The scale bar is 200 nm. (b) Voltammetric response of such nanotubes in the absence (lower curves) and presence (upper curves) of the substrate, β-D-glucose. (TMAFM = tapping-mode atomic force microscopy). (Reprinted with permission from Ref. [70]. © 2003 Wiley-VCH.)

layers was recently provided for DNA sensing [74]. By applying an impedance technique to this two-layer-based sensor, the complementary DNA target can be detected down to 5×10^{-11} M.

Sol–gel chemistry involves the hydrolysis and condensation of suitable alkoxysilane precursors and has been widely employed for the preparation of inorganic materials (monolithic, hybrid, composites, and chromatographic stationary phase) suitable for various applications. Recently, Bachas and coworkers have applied a CNT sol–gel composite as an enzyme-friendly platform to develop biosensors [75]. Using L-amino acid oxidase as a model enzyme, the biosensors were made in aqueous sol–gel processes involving methyltrimethoxysilane, ethyltrimethoxysilane and propyltrimethoxysilane as precursors. Aliquot amounts of MWCNTs and enzyme were added into the sol when the hydrolysis took place. The resultant sensor proved to be stable and retained more than 50% of its response after 1 month of testing. In such an immobilization protocol, the porous –Si–O– sol–gel network

encapsulates biomolecules while the use of CNTs, as the conductive part of the composite, facilitated fast electron transfer rates.

Because of the unique sp^2 hybrid surface structures, CNTs themselves could be viewed as an extreme form of conducting polymer. The CNT bulky material may be applied directly towards sensor construction without binders or other auxiliary components. Wang and co-authors have developed a simple approach for preparing effective CNT-based biosensors from CNT/Teflon composite material by hand-mixing a certain amount of CNTs in the dry-state with granular Teflon to obtain a desired composition of CNT/Teflon [76]. Carbon composites, based on the dispersion of graphite powder within an insulator, offer convenient bulk modification for the preparation of reagentless and renewable biosensors. Wang et al.'s approach relies on CNTs as the sole conductive component rather than as the modifier cast on other electrode surfaces. The bulk of CNT/Teflon composites hence serve as a reservoir for the enzymes. By comparing the sensors' performance against their respective composite compositions, the CNT content of 40–60 wt.% has been suggested. CNT/Teflon composites combine advantages of CNTs and bulk composite electrodes that permit a wide range of applications without the need for a graphite surface. Certain amounts of enzymes (e.g., glucose oxidase and alcohol dehydrogenase) and cofactor (e.g., NAD^+) can be mixed with the CNT/Teflon composite and used as electrode materials, depending upon specific needs. These biosensor interfacings displayed a marked electrocatalytic action toward hydrogen peroxide and β-nicotinamide adenine dinucleotide (NADH) and, hence, this is promising for the development of biosensors for glucose (in connection with oxidase enzymes) and ethanol (in connection with dehydrogenase enzyme), respectively [76]. Similar approaches have been developed for CNT-based sensor fabrication using nanotube–mineral oil paste, reagent-embedded CNT paste, or powders to determine DNA, glucose, cysteine, and other biomolecules.

Composites consisting of CNTs and other nanotubes or nanoparticles were reported recently for enhancing the catalytic capacity of the sensing devices. Luong's group [77] and Yao's group [78] used platinum nanoparticles combining with CNTs to construct a biosensing platform for glucose oxidase. Wang et al. employed semiconductor CdS nanoparticle-tagged CNTs for DNA hybridization detection [79].

3.2.2.7 More Sophisticated Surface Tailoring Based on Combination of Co-adsorption, Integration, Prohibition, Spacing, Linkage, Sandwich, Tagging, and other Anchoring Approaches

Biosensors involve biomolecules and biorecognition reactions. Their optimal operational performance depends on the maximization of the desired signals while minimizing the side reaction. DNAs, enzymes, antigens, and other biomolecules usually bear charges, depending on the medium pH. CNT biomodifications based on non-specific interaction with DNAs or proteins can be achieved through the sidewall electrostatic interaction, hydrogen bonding, and other mechanisms, as well as the insertion of smaller biomolecules into the tubular channel. The nature of these noncovalent bondings are complicated and were proposed by Dai et al. as

mainly the results of hydrophobic interaction and the π-stacking of the conjugated pyrenyl group of 1-pyrenebutanoic, succinimidyl ester, or coating with some surfactants, such as Triton [80, 81]. More specific binding to functionalize the CNTs can take advantage of covalent bonding, DNA hybridization, coupling agents, and antigen–antibody interactions. Biosensing by these approaches was reported for the CNTs attachment of decorated glucose oxidase [82], thiolated DNA [83], amine-terminated DNA [84], and peptide nucleic acid (PNA) – a DNA mimic [85].

The non-specific adsorption of proteins on nanotubes is not always desirable, especially when tested in real biofluid samples that contain many co-existing proteins. More sophisticated sensors, therefore, need to address issues like target-recognition enhancement, blockage of undesired interference (the co-existing proteins' non-specific adsorption on the nanotube surfaces), long-term storage, etc. Accordingly, CNT surface engineering might be a combination of different tailoring techniques. Dai et al. have presented a typical example [81] (Fig. 3.4). In their approach U1A, a protein involved in the splicing of message ribonucleic acid (mRNA), was covalently linked to Tween-20, a surfactant. The complex was then noncovalently cast onto the single-walled CNT surface. The latter was as-grown on a quartz wafer that was *in situ* monitored by its conductance and frequency response during the sensing measurement.

This CNT modification with the adsorption of biotinylated Tween-20 allowed streptavidin recognition by the specific biotin–streptavidin interaction, but provided resistance toward other protein adsorptions. Under such design, the sensor could detect the binding of 10E3, a specific antibody for recognition of U1A, at concentrations as low as 1 nM (Fig. 3.4), while showing no response toward other existing proteins such as streptavidin, avidin, bovine serum albumin (BSA), a-glucosidase, staphylococcal protein A (SpA), and immunoglobulin G (IgG) (Fig. 3.4C). The blocking mechanism toward coexisting proteins was proposed as the formation of a nearly uniform layer of surfactant Tween-20 through the favorable hydrophobic interaction on the nanotube surface, with the poly(ethylene glycol) (PEG) segments extending into the aqueous media to provide the observed protein resistance. Noticeably, this protein-resistant assembly may be covalently conjugated to specific antigens to allow sensitive detection of antibodies, or *vice versa* [81]. This proposed real-time immunosensor can thus compare favorably with a standard fluorescence-based assay with immobilized antigens on planar arrays.

Wang et al. have recently developed a CNT-based amplified bioelectronic protocol that uses DNA for linking particles to CNTs [63]. As can been seen in Fig. 3.5(a), the preparation is based on the sandwich hybridization (a) or antigen–antibody (b) binding along with magnetic separation of the analyte-linked magnetic-bead/CNT assembly (A), followed by enzymatic amplification (B), and chronopotentiometric stripping detection of the product at the CNT-modified electrode (C). TEM observations (Fig. 3.5D) indicate that the hybridization event leads to crosslinking of the alkaline phosphatase (ALP)-loaded CNTs and the magnetic beads (with the DNA duplex acting as "glue"). In this new bioaffinity assay, CNTs play a dual amplification role in both the recognition and transduction events, namely as carriers for

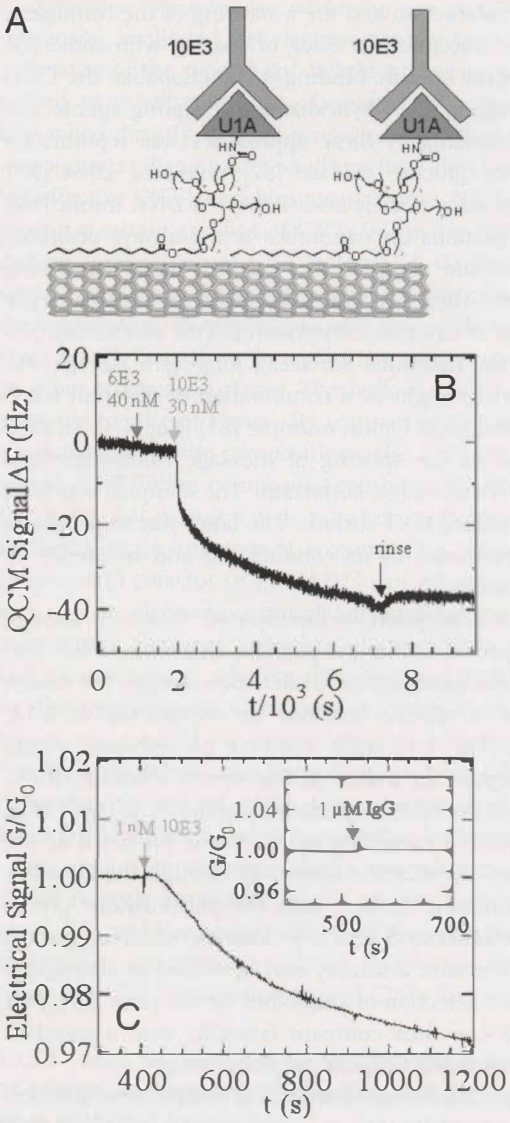

Fig. 3.4. Specific detection of mAbs binding to a recombinant human autoantigen. (A) Scheme for specific recognition of 10E3 mAb with a nanotube device coated with a U1A antigen–Tween conjugate. (B) QCM frequency shift vs. time curve showing selective detection of 10E3 while also showing rejection of the antibody 6E3, which recognizes the highly structurally related autoantigen TIAR. (C) Conductance vs. time curve of a device, revealing a specific response to ≤1 nM 10E3 while rejecting polyclonal IgG at a much greater concentration of 1 μM (inset). (Reprinted with permission from Ref. [81]. © 2003 of National Academy of Sciences, U.S.A.)

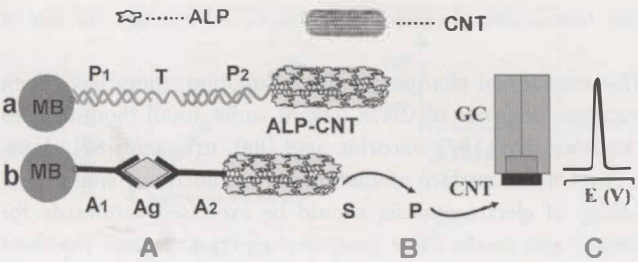

Fig. 3.5. Schematic representation of the analytical protocol: (A) Capture of the ALP-loaded CNT tags to the streptavidin-modified magnetic beads by a sandwich DNA hybridization (a) or Ab-Ag-Ab interaction (b). (B) Enzymatic reaction. (C) Electrochemical detection of the product of the enzymatic reaction at the CNT-modified glassy carbon electrode. (D) TEM image of the magnetic beads-DNA-CNT assembly produced following a 20-min hybridization with the 10 pg mL^{-1} target sample. Micrographs were taken with a Hitachi H7000 instrument operated at 75 kV after washing the DNA-linked CNT/particle assembly with autoclaved water, placing a 5-μL drop of the aggregate sample onto a carbon-coated copper grid (3 mm diameter, 200-mesh), and allowing it to dry. MB, Magnetic beads; P_1, DNA probe 1; T, DNA target; P_2, DNA probe 2; Ab_1, first antibody; Ag, antigen; Ab_2, secondary antibody; S and P, substrate and product, respectively, of the enzymatic reaction; GC, glassy carbon electrode; CNT, carbon nanotube layer. (Reprinted with permission from Ref. [63]. © 2003 American Chemical Society.)

numerous enzyme tags and for accumulating the product of the enzymatic reactions. With such an assembly, the extraordinarily low detection limits were reported for DNA and IgG of 1 and 500 fg mL^{-1}, respectively.

3.2.3 CNT-based Electrochemical Biosensors

Soluble CNTs have been electrochemically and quantum-chemically characterized for their bulk properties [86]. Results showed that the electronic states are not strongly affected when the nanotubes are functionalized. The electronic properties of CNTs range from metallic to semiconductive, depending on the nanotube's own diameter and chirality. These subtle electronic properties offer various electrochemical features for CNT-based sensors after functionalization of the nanotubes.

3.2.3.1 Direct Electrochemistry of Biomolecules on Carbon Nanotubes

Recently, direct electrochemical communications between redox-active macrobiomolecules and conventional electrode substrates mediated by CNTs have received attention because of their potential to lead a mechanistic study of the structure–function relationship of these biomolecules and their guidance toward biosensor design. Wang et al. reported the direct electrochemistry of cytochrome *c* at electrochemically activated SWCNT-modified electrodes [23]. Gooding et al. and Rusling et al. have used aligned nanotubes to promote the direct electrochemistry of redox-active proteins [66, 67]. These studies demonstrate that direct electro-

chemistry of redox-active biomacromolecules can be improved through the use of CNTs.

In addition to the aforementioned charge transfer promotion, there have been reports on the electrocatalytic behavior of CNTs toward some small biomolecules such as cysteine and hemocysteine [87], ascorbic acid [88], uric acid [89], dopamine [90]. The mechanisms of this surface mediation are not currently well understood, and the terminology of electrocatalysis should be exercised cautiously for different electrode material and media. The promoted electrochemical reactions for hydrogen peroxide, NADH, and quinones enable possible sensing schemes for more than 800 enzymes that involve these substrates, products, coenzymes, and cofactors.

Several hundred enzymatic reactions of NAD^+/NADH-dependent dehydrogenases have NADH as a cofactor. The electrochemical oxidation of NADH has thus been the subject of numerous studies related to the development of amperometric biosensors. Problems inherent to such anodic detection are the large overpotential encountered for NADH oxidation at ordinary electrodes and surface fouling associated with the accumulation of reaction products. CNTs have thus been examined in recent work [91] as the new electrode material to alleviate these problems.

Lin et al. have employed CNTs that had been pretreated with dispersion in concentrated sulfuric acid to cast a glassy carbon electrode [91]. Figure 3.6 shows a typical hydrodynamic voltammogram of 1×10^{-4} M NADH in a physiological medium (0.05 M phosphate solution, pH 7.4). This voltammogram demonstrates an electrocatalytic behavior of the CNT coating towards NADH with varying potentials, as evidenced by the MWCNT-coated electrode (B) responding to NADH over

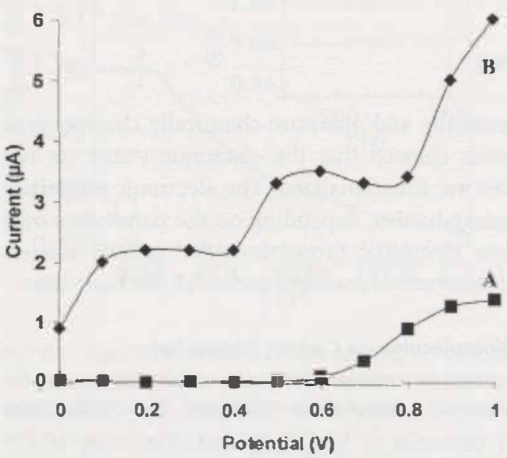

Fig. 3.6. Hydrodynamic voltammograms for 1×10^{-4} M NADH at unmodified (A) and MWCNT-modified (B) GC electrodes. Operating conditions: stirring rate, 500 rpm; electrolyte, phosphate buffer (0.05 M, pH 7.4). (Reprinted with permission from Ref. [91]. © 2002 Elsevier.)

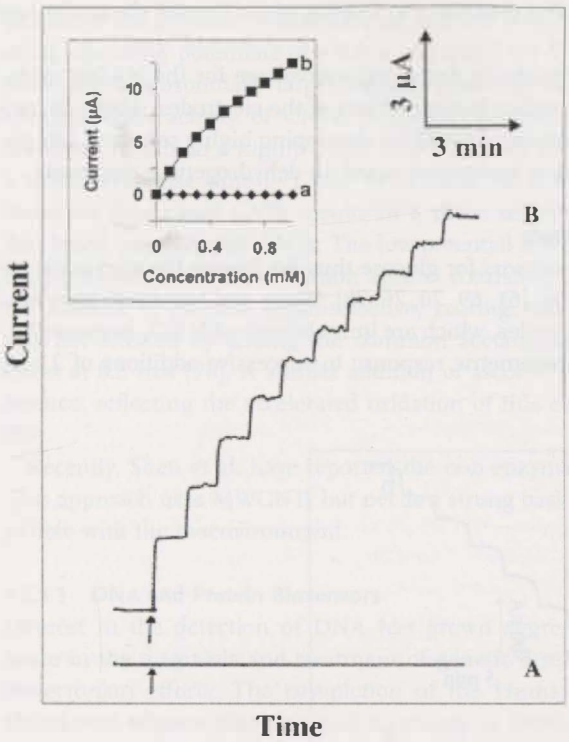

Fig. 3.7. Current–time recordings obtained after increasing the NADH concentration (by 1×10^{-4} M at each step) at unmodified (A) and MWCNT-modified (B) GC electrodes. Inset: the corresponding calibration curve. Operating conditions: potential, +0.3 V. (Reprinted with permission from Ref. [91]. © 2002 Elsevier.)

the entire 0.0–1.0 V range, whereas the bare electrode (A) responds only at potentials higher than +0.6 V. The modified electrode yields an approximately three-fold larger NADH peak than does the unmodified electrode. Figure 3.7 shows that successive additions of 1×10^{-4} M NADH result in increasing response detected at the CNT-modified electrode (B) but no response at the unmodified electrode (A) when the detection potential was kept low (i.e., 0.3 V). Evidently, the electrocatalytic action of CNT enables the fast response (i.e., 10 s to reach the steady state) to the change of NADH concentrations at the low-detection potential. The amperometric response of 5×10^{-3} M NADH appears to be very stable; the decay of the signal is less than 10% and 25% after a 60-min period at the MWCNT-modified and SWCNT-modified electrodes, compared with 75% and 53% at the graphite-coated and acid-treated electrodes, respectively. This shows the capability of CNTs to resist the fouling effects and prevent the diminishing of signals in successive cyclic voltammetric detections. The oxygen-rich groups on the CNT surface, introduced during the acid dispersion, are perhaps responsible for such electrocatalytic behavior

for the oxidation of NADH. The resistance to fouling of CNT-based electrodes has yet to be understood.

The CNT-coating offers remarkably decreased overvoltage for the NADH oxidation as well as reducing the surface fouling effects of the electrodes. These characteristics indicate the great promise of CNTs for developing highly sensitive, low potential, and stable amperometric biosensors based on dehydrogenase enzymes.

3.2.3.2 Enzyme/CNTs Biosensors

Most reported CNT-based biosensors for glucose thus far involve the enzymatic reaction by glucose oxidase (GOx) [61, 69, 70, 76, 78]. Wang and Musameh have employed CNT/Teflon-based electrodes, which are immobilized with GO_x enzyme [76]. Figure 3.8 compares the amperometric response to successive additions of 2 mM

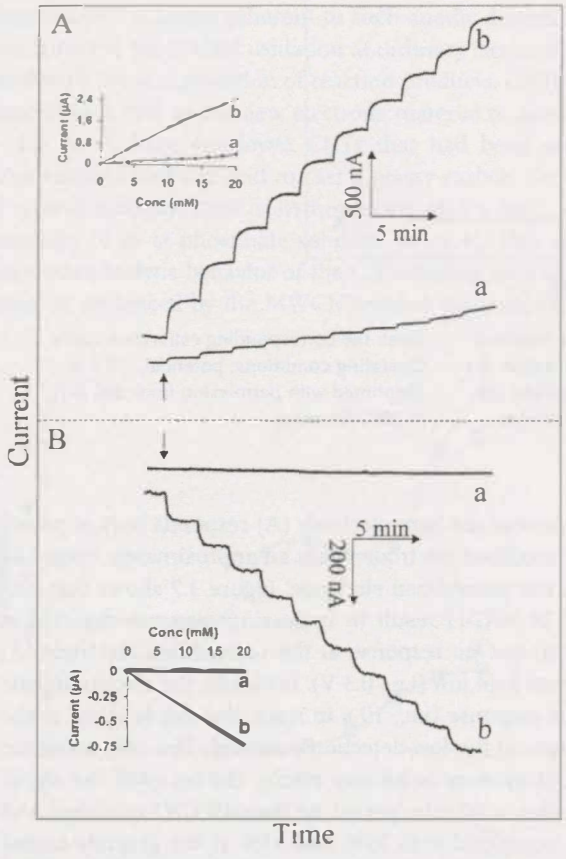

Fig. 3.8. Current–time recordings for successive 2-mM additions of glucose at graphite/Teflon/GO_x (a) and the MWCNT/Teflon/GO_x (b) electrodes measured at +0.6 (A) and +0.1 V (B). Electrode composition, 30:69:1 wt.% carbon/Teflon/GO_x. (Reprinted with permission from Ref. [76]. © 2003 American Chemical Society.)

glucose at the graphite/Teflon/GO_x (a) and the MWCNT/Teflon/GO_x (b) electrodes using operating potentials of +0.6 V (A) and +0.1 V (B). The CNT-based bioelectrode offers substantially larger signals, especially at low potential, reflecting the electrocatalytic activity of CNTs. Such low-potential operation of the CNT-based biosensor results in a highly linear response (over the entire 2–20 mM range) and a slower response time (~1 min vs. 25 s at +0.6 V). The glucose biocomposite based on single-wall CNTs results in a more sensitive but slower response than that based on multiwall CNTs. The low-potential detection also leads to high selectivity (i.e., effective discrimination against coexisting electroactive species). Despite the absence of external (permselective) coating, the glucose response at +0.1 V was not affected by adding the common acetaminophen and uric acid interferences at 0.2 mM [76]. A similar addition of ascorbic acid resulted in a large interference, reflecting the accelerated oxidation of this compound at the CNT surface [88].

Recently, Sheu et al. have reported the non-enzymatic detection of glucose [92]. This approach uses MWCNTs but needs a strong basic media that may not be compatible with the bioenvironment.

3.2.3.3 DNA and Protein Biosensors

Interest in the detection of DNA has grown aggressively because of its importance in the diagnosis and treatment of genetic disease, drug discovery, and antibioterrorism efforts. The completion of the Human Genome Project offers an abundance of gene mapping and screening. A hybridization recognition scheme, based on the Watson–Crick base pair principle, is the central point when constructing a DNA sensor. The unique electric, thermal, chemical, mechanical, and 3D spatial properties of CNTs make them a natural choice as transducers for hybridization-based DNA sensors. Different attachment protocols for DNA probes (single strand DNA molecules) onto CNTs were introduced, either by unmodified or surface-confined nanotubes [40, 63, 93].

Wang and coworkers have developed an ultrasensitive DNA biosensor based on a "dual amplification route" by using CNTs both as recognition sites and transducers, namely as carriers for numerous enzyme tags and for accumulating the product of the enzymatic reaction [63]. Figure 3.9 displays typical chronopotentiograms for extremely low target DNA concentrations (0.01 to 100 pg mL^{-1}; a–e). Well-defined α-naphthol signals are observed for these low DNA concentrations in connection with 20-min hybridization. The resulting plot of response vs. log[Target] (shown as inset) is linear and suitable for quantitative work. The favorable response of the 5 fg mL^{-1} DNA target (B) indicates a remarkably low detection limit of around 1 fg mL^{-1} (54 aM), i.e., 820 copies or 1.3 zmol in the 25-μL sample. Such a low detection limit compares favorably with the lowest values of 5 zmol (3000 copies) and 25 amol reported for electrical DNA detection. The smaller signal observed in a control experiment for a huge (~10^6) excess of a noncomplementary oligonucleotide (Fig. 3.9C vs. B) reflects the high selectivity associated with the effective magnetic separation. The amplified electrical signal is coupled to a good reproducibility. Two series of six repetitive measurements of

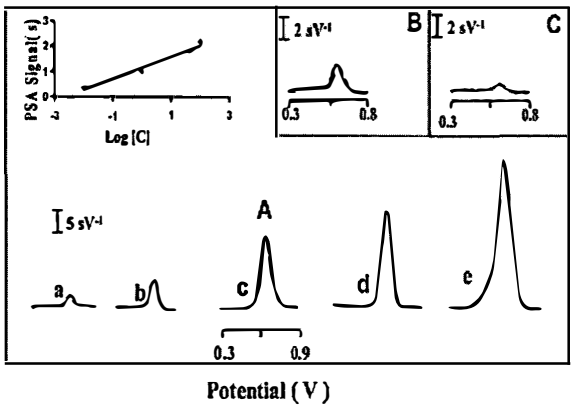

Fig. 3.9. Chronopotentiometric signals for increasing levels of the DNA target: (a) 0.01, (b) 0.1, (c) 1, (d) 50, (e) 100 pg mL^{-1}. Also shown (inset) is the resulting calibration plot (A), and the response for 5 fg mL^{-1} target DNA (B) and 10 ng mL^{-1} non-complementary (NC) oligonucleotide (C). Sample volume, 25 (B) and 50 μL (C). (Reprinted with permission from Ref. [63]. © 2003 American Chemical Society.)

1 pg mL^{-1} DNA target or 0.8 ng mL^{-1} IgG yielded reproducible signals with relative standard deviations of 5.6% and 8.9%, respectively [63].

Noticeably, Wang's "dual amplification" mode for the DNA sensor as above has also been applied to an immunosensor for IgG because of the similarity between DNA hybridization and antigen–antibody interaction. An extremely low detection for IgG was reported, as 500 fg mL^{-1} [63]. In contrast, DNA, RNA, proteins, and enzymes all bear multiple charges, and their adsorption onto the nanotubes is expected to change their electronic properties. These changes, upon adsorption, can be readily transduced into measurable sensing signals [38, 94]. DNA has already been used as a template to localize CNTs to make new building blocks or alignments in electronics and bioelectronics, such as field-effect transistors (FETs) [95]. These functionalized FETs, coupled with advanced sensor array techniques, can therefore serve as a new direction in CNT-based bioassays [77, 80].

3.2.3.4 Immunosensors

Electrochemical immunosensors based on CNTs have been designed [20]. Vertically aligned arrays of single CNTs called SWCNT forests have been developed for amperometric enzyme-linked immunoassays of proteins by Rusling and coworkers [20]. A prototype amperometric immunosensor was evaluated based on the adsorption of antibodies onto perpendicularly oriented assemblies of SWCNT forests. The forests were self-assembled from oxidatively shortened SWCNTs onto Nafion/iron oxide coated pyrolytic graphite electrodes. Anti-biotin antibodies strongly adsorbed to the SWCNT forests. They found that the detection limit for horseradish peroxidase (HRP) labeled biotin was 2.5 pmol mL^{-1} (2.5 nM) in the presence of a soluble mediator. Unlabeled biotin was detected in a competitive approach with a detection

limit of 16 nmol mL^{-1} and a relative standard deviation of 12%. The immunosensor showed low non-specific adsorption of biotin-HRP (approx. 0.1%) when blocked with bovine serum albumin. The biosensor platform is also being developed to accommodate flow-through sensor design with direct electron transfer detection of the enzyme label on a CNT matrix. Traditional electrochemical immunosensors were based on mediated electron transfer. However, efficient direct electron transfer will offer some advantages, such as a simple possibility for a reagentless immunoassay. CNTs exhibit excellent electrical properties, and they are a suitable candidate for developing such a reagentless immunoassay.

3.2.4 Flow-injection Analysis

Flow detectors have been widely used in process chemistry and online monitoring. It is the core part for real time, *in situ* analysis and for the integration of separation and detection – "lab-on-a-chip." Microfabricated fluidic devices, particularly used as sensors for capillary electrophoresis (CE) and liquid chromatography (LC), have gained steadily growing attention in recent years [64]. Wang et al. have presented a CNT-based detector for a conventional as well as a miniaturized CE system [64]. CE combines the advantages of high performance, design flexibility, reagent economy, high throughput, miniaturization, and automation. It demands a detector with high sensitivity, inherent miniaturization (of both the detector and control instrumentation), and compatibility with advanced micromachining technologies, and low cost and power requirements [64]. Conventional detectors are based on gold, platinum, and various forms of carbon. A CNT-based electrode offers an alternative for low potential detection, it imparts enhanced sensitivity, and it leads to long-term stability. In this approach, Wang et al. used a Nafion/CNT-coated screen-printed electrode for end-column amperometric detection. After anodic pretreatment (3 min at +1.5 V in 1 M sulfuric acid), this sensor showed substantial electrocatalytic behavior and resistance to surface fouling toward hydrazine, phenol, tyrosine, purine, and amino acids, when compared with the bare surface. The CNT microchip detector also displayed well-defined concentration dependence.

Typical flow detection for glucose, based on the CNT/Nafion/GO_x modified gas chromatography (GC) electrode, can be seen in Fig. 3.10 (from the work by Wang's group) [61]. Figure 3.10 compares the amperometric responses for relevant physiological levels of glucose, ascorbic acid, acetaminophen, and uric acid at the CNT/Nafion/GO_x modified GC electrode (B) and Nafion/GO_x modified GC electrode (A). In Figure 3.10, the accelerated electron-transfer reaction of hydrogen peroxide at the CNT/Nafion/GO_x modified GC electrode allows for glucose measurements at very low potentials (i.e., −0.05 V) where interfering reactions are minimized. As a result, a well-defined glucose signal (d) is observed, while the signals of acetaminophen (a), uric acid (b), and ascorbic acid (c) are negligible. No such discrimination is obtained at the Nafion/GO_x biosensor (without the CNT) (A) held at +0.80 V, where large oxidation peaks are observed for all interferences, indicating that the permselective (charge exclusion) properties of Nafion are not adequate to

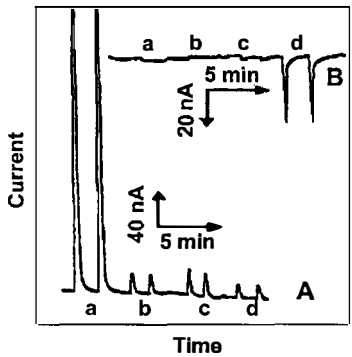

Fig. 3.10. Flow-injection signals for 2×10^{-4} M acetaminophen (a), 2×10^{-4} M ascorbic acid (b), 2×10^{-4} M uric acid (c), and 1×10^{-2} M glucose (d) at a Nafion/GO_x-modified GC electrode (A) at +0.8 V, and at a MWCNT/Nafion/GO_x-modified GC electrode (B) at −0.05 V, and flow rate of 1.25 mL min^{-1}. (Reprinted with permission from Ref. [61]. © 2003 American Chemical Society.)

fully eliminate anionic interferences. In short, the coupling of the permselective properties of Nafion with the electrocatalytic action of CNT allows for glucose detection with effective discrimination against both neutral and anionic redox constituents. Similarly, the CNT/Nafion-coated electrodes have also been demonstrated to dramatically improve the signal of dopamine in the presence of the common ascorbic acid interference [61].

Jin et al. used CNT-based sensors for LC detection [97, 98]. To overcome the aggregation of nanotubes in aqueous and common organic solution, nitric acid was used to treat CNTs to introduce carboxyl groups in the open ends of the MWCNTs. Such functionalized CNTs were cast onto the glassy carbon as the flow detector. Various biofluids containing neurotransmitters were tested using this protocol. The results from real samples such as plasma agreed with those from other methods.

In terms of the mechanism of the CNT-based flow sensor, Ghosh et al. recently found that the flow of a liquid on single-walled CNT bundles induces a voltage in the sample along the direction of the flow [98]. The magnitude of the voltage depended sensitively on the ionic conductivity and on the polar nature of the liquid. The nonlinear response of flow velocity and the voltage was attributed to a direct forcing of the free charge carriers in the nanotubes by the fluctuating Coulombic field of the liquid flowing past the nanotubes. Their work highlighted the potential of a CNT-based device as sensitive flow sensors and for energy conversion [98].

3.2.5
Carbon Nanotube Array-based Biosensors

Control over the orientation, distribution, and effective sensing sites of the nanotubes have been the subject of CNT-based biosensor research [56, 66]. Several ap-

proaches have been reported to achieve these controlled-density aligned CNTs and CNT arrays. The versatile approach is that of self-assembling aligned nanotube arrays by using oxidative acid treated single walled nanotubes [99]. These shortened tubes then react with DCC to introduce a carbodiimide leaving a group that allows reaction with thiols. Finally, these thiolated nanotubes are self-assembled on the gold surface to form aligned CNT arrays. Alternatively, aligned CNT arrays can be grown off a surface by using pyrolyzing CVD of relevant catalysts and carbon materials, followed by transferring the tubes onto a substrate support [73]. The third approach is to grow directly aligned CNTs onto an electrode surface by using CVDs or plasma, offering a controllable size and a given location for the catalyst spots that allows the growth of a given numbers of nanotubes [93].

Although vertically aligned CNTs have good material properties (e.g., good electrical conductivity, the capability to promote electron transfer reactions) and are of the right size (20 to 200 nm) for nanoelectrode arrays (NEAs), they lack the right spacing, having little support, and, therefore, the electrodes may lack robustness. To make each nanotube work as an individual nanoelectrode, the spacing needs to be sufficiently larger than the diameter of the nanotubes to prevent diffusion layer overlap from the neighboring electrodes [100]. Ren and co-authors recently developed a nonlithography method that allows the fabrication of low site density aligned CNT arrays with an interspacing of more than several micrometers [101]. Figure 3.11 demonstrates the manufacturing process of such aligned CNT arrays: Ni nanoparticles were randomly deposited on a 1-cm^2 Cr-coated silicon substrate

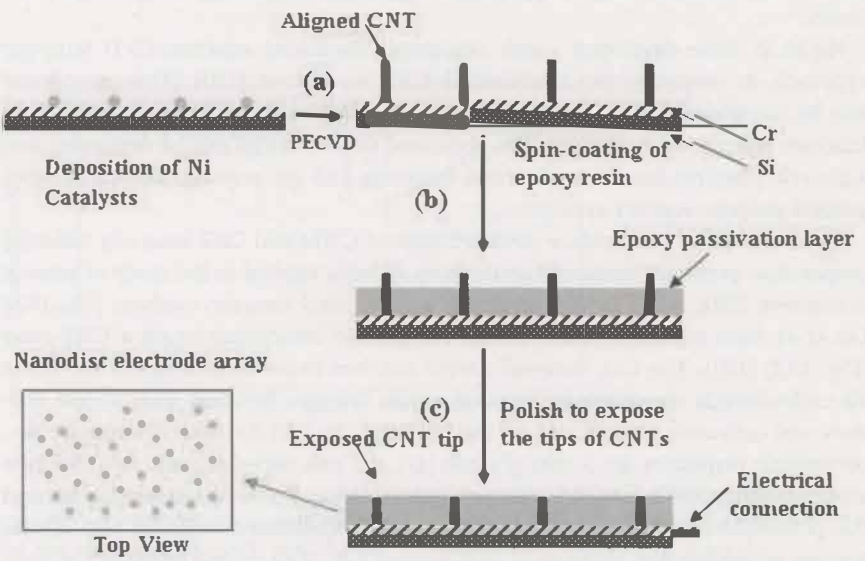

Fig. 3.11. Fabrication scheme of a low-site-density aligned CNT nanoelectrode array. (Reprinted with permission from Ref. [101]. © 2003 American Chemical Society.)

(Fig. 3.11a) by applying a pulse current to the substrate in a $NiSO_4$ electrolyte solution. The size and the site density of the Ni nanoparticles were controlled by the amplitude and the duration of the pulse current. On these Ni particles, the CNTs were grown (Fig. 3.11b) in the plasma-enhanced chemical vapor deposition (PECVD) system at 650 °C for 8 min with 160 sccm NH_3 and 40 sccm C_2H_2 gases with a total pressure of 15 Torr and a plasma intensity of 170 W. The aligned CNT arrays had a site density of 1×10^6–3×10^6 cm^{-2}, a length of 10 to 12 μm, and a diameter of 50–80 nm. A thin layer of Epon epoxy resin 828 (Miller-Stephenson Chemical Co., Inc., Sylmar, CA) was coated on the surface by magnetron sputtering to insulate the Cr layer. This was followed by applying m-phenylenediamine (MPDA) as a hardener. After these steps, the CNTs were half-embedded in the polymer resin, and the protruding part of the CNTs beyond the polymer resin was mechanically removed by polishing with a lens, followed by ultrasonication in water. Then the electronic connection was made on the CNT-Si substrate to make the CNT nanoelectrode arrays (Fig. 3.11c). Finally, the electrode arrays were pretreated by electrochemical etching in 1.0 M NaOH at 1.5 V for 90 s before electrochemical characterizations [101]. Results showed that, within these low site density CNTs, the NEAs consist of millions of nanoelectrodes, with each electrode being less than 100 nm in diameter. There is no degradation of these sensors for several weeks because of the excellent stability of the epoxy layer. Since the total current of the loosely packed electrode arrays is proportional to the total number of individual electrodes, having the number of the electrodes up to millions is highly desirable. The size reduction of each individual electrode and the increased total number of the electrodes result in improved signal-to-noise ratio (S/N) and detection limits.

Ng et al. have developed a soft lithography-mediated selective CVD template approach in preparing the multiwalled CNT membrane [102]. This membrane can be integrated with a flexible elastomeric polydimethylsiloxane framework to fabricate microsensing devices. The presented sensor design can be developed into a generic platform for electrochemical detection and gas sensing, as well as other general purpose sensory systems.

The unmodified and surface-confined aligned CNTs and CNT arrays by different preparation protocols discussed above have all been applied to the study of protein interaction [101, 103], DNA hybridization [104], and enzyme catalysis [66, 102]. Lin et al. have reported typical results for glucose biosensing using a CNT array (Fig. 3.12) [103]. The GO_x molecules were attached to the broken tips of the CNTs via carbodiimide chemistry by forming amide linkages between their amine residues and carboxylic acid groups on the CNT tips. Fig. 3.12(a) and (b) compare amperometric responses for 5 mM glucose (G), 0.5 mM ascorbic acid (AA), 0.5 mM acetaminophen (AC), and 0.5 mM uric acid (UA) at the GO_x-modified NEA and the potentials of +0.4 V (a) and −0.2 V (b). Well-defined cathodic and anodic glucose responses are obtained at this aligned CNT/GO_x-based biosensor at both potentials. However, the glucose detection at a lower operating potential (−0.2 V) is significantly less influenced by the interferences, indicating high selectivity towards the glucose substrate. Such a highly selective response to glucose is obtained

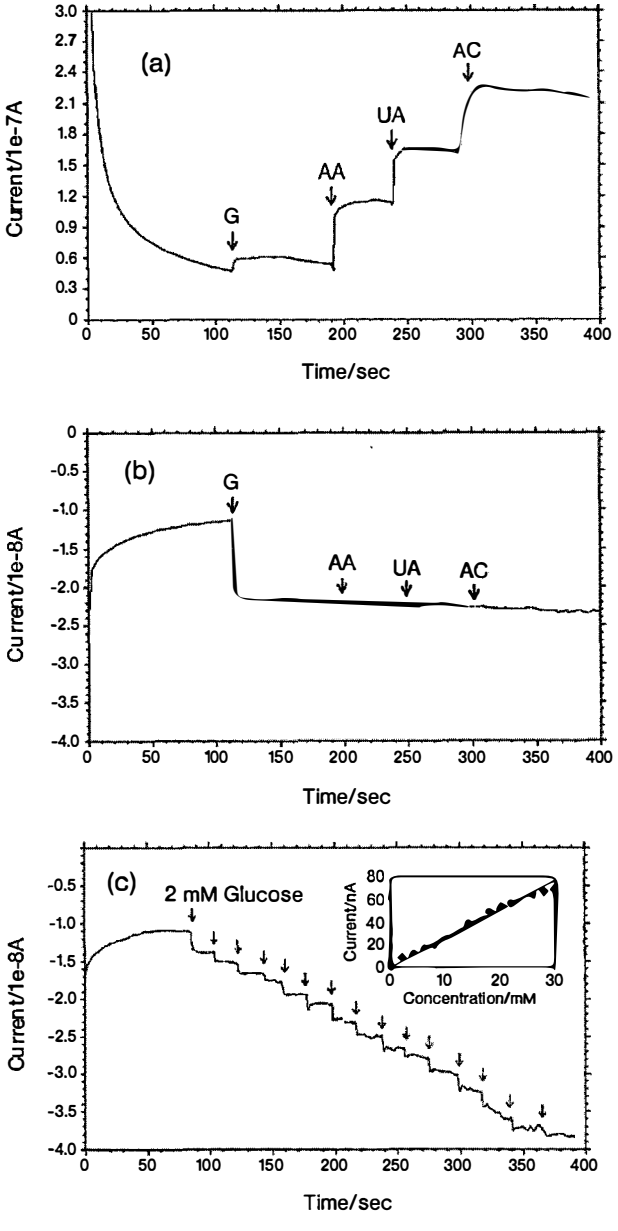

Fig. 3.12. (a, b) Amperometric responses for 5 mM glucose (G), 0.5 mM ascorbic acid (AA), 0.5 mM acetaminophen (AC), and 0.5 mM uric acid (UA) at a GO_x-modified, CNT-nanoelectrode array and potentials of +0.4 (a) and −0.2 V (b). Electrolyte: 0.1 M phosphate buffer/0.1 M NaCl (pH 7.4). (c) Amperometric response at the GO_x-modified, CNT-nanoelectrode array for each successive addition of 2 mM glucose. Inset: the corresponding calibration curve. Potential: −0.2 V, other conditions are as in (a, b). (Reprinted with permission from Ref. [103]. © 2003 American Chemical Society.)

at this aligned CNT/GO_x-based biosensor without the use of mediators and permselective membranes. The amperometric response at this sensor for each successive addition of 2×10^{-3} M glucose is presented in Fig. 3.12(c) with the corresponding calibration curve in the inset. The linear response to glucose is up to 30 mM, and steady state is reached within 20 to 30 s [103]. Because of this low potential detection, CNTs eliminate perspective interferences through the preferential detection of hydrogen peroxide at the CNT-based electrodes. Such development of interference-free transducers will significantly simplify the design and fabrication of biosensors. Biosensors based on low-site-density aligned CNTs are also suitable for the highly selective detection of glucose in various biological fluids (e.g., saliva, sweat, urine, and serum) [103].

Rusling et al. reported the first example of enzymes covalently attached onto the ends of vertically oriented SWCNT forest arrays [67]. These arrays were made from their unique methodology of assembling dense orthogonally oriented arrays of shortened SWCNTs. Quasi-reversible Fe^{III}/Fe^{II} voltammetry was obtained for the iron heme enzymes myoglobin and horseradish peroxidase coupled to the carboxylated ends of the nanotube forests by amide linkages. Their observation suggested that the "trees" in the nanotube forest behaved, electrically, similarly to a metal, conducting electrons from the external circuit to the enzymes. Accordingly, the electrochemically manifested peroxidase activity of myoglobin and horseradish peroxidase attached to the CNT array was demonstrated, showing analytical promise for hydrogen peroxide with a detection limit down to ~100 nM in buffer solutions. The covalently attached enzymes kept their activity for weeks in these prototype SWCNT-forest array biosensors [67]. Gooding and co-authors also observed the direct charge transfer between redox-active enzymes and the aligned CNTs' surface [66]. Their mechanistic study revealed that the rate of electron transfer remains the same regardless of the lengths of the tubes. These findings enable electroactive molecules to be located several hundred nanometers from a macroscopic substrate electrode with no loss in performance. This might guide future modification of the CNT array for sensor applications.

While most of the array studies have focused on their electrochemical mode, because of the unique electronic properties of individual nanotubes and nanotube arrays, optical sensing based on CNT arrays has also been carried and has been reviewed by Xu [21].

3.2.6 Chemiluminescence

Miscellaneous CNT sensing applications have been reported recently by using different transducer techniques with various nanotube platforms. As a traditional technique, fluorescence spectroscopy has been widely employed in sensor and bioassay application because of its high sensitivity. However, there have been few reports regarding its study on CNTs, partly because of the limited aqueous solubility or dispersion of CNTs [105, 106]. By using amine-terminated oligonucleotide-functionalized CNTs, Hazani and co-authors were able to enhance nanotube solu-

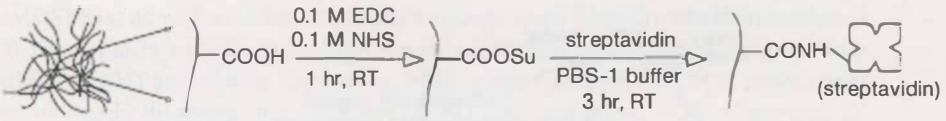

Fig. 3.13. Reaction scheme of immobilization of streptavidin on nanotubes by covalent coupling. (Reprinted with permission from Ref. [105]. Copyright 2003 Wiley-VCH.)

bility to facilitate the confocal fluorescence imaging of the DNA hybridization from a fluorescence dye-tagged complementary sequence [107]. Baker et al. used thiol-terminated oligonucleotide-modified CNTs for the similar assay [108].

A more direct application of CNT based biosensors has been reported by Wohlstadter et al. in their electrogenerated chemiluminescence (ECL) study of immunoassays for α-fetoprotein (AFP) [105]. Nanotubes possess several characteristics that make them attractive for ECL-based assays: First, they are conductive or semiconductive and hence can act as electrodes to generate ECL in aqueous solutions; second, nanotubes can be surface-functionalized as we discussed before; finally, their high surface area-to-volume ratio and sp^2 network make them feasible for immobilizing biomolecules as well as their associated electrochemistry. Wohlstadter et al. first mixed nanotubes with poly(vinyl acetate) (EVA) to form a nanotube–EVA composite. This composite was then etched with strong acid to produce a densely packed nanotube sheet with available surface carboxylic acid groups. As can be seen in Fig. 3.13, streptavidin was then immobilized on the nanotube sheet by carbodiimide-activated coupling, followed by the attachment of a biotinylated mAb for AFP via the specific biotin–streptavidin interaction. Figure 3.14 shows the whole assay based on this sensor. The capture of AFP resulted in the binding of a $Ru(bpy)_3^{3+}$ labeled antibody on to the EVA-MWCNTs composite electrode. As the $Ru(bpy)_3^{3+}$ is chemiluminescent, binding is transduced by the release of light upon applying the electrode at potentials more positive than +1 V. This immunosensor with electrochemiluminescence detection was sensitive at AFP concentrations as low as 0.1 nM, with a linear range up to 30 nM [105].

By using chemiluminescent $Ru(bpy)_3^{3+}$ as a marker, Dong et al. found that the CNT/Nafion composite possesses ECL sensitivity two orders of magnitude more than that at the silica/Nafion composite and three orders of magnitude more than that at pure Nafion films, again proving that the solubility enhancement for CNTs plays a key role in developing a CNT-based fluorescence sensor [106].

3.2.7
Field-effect Transistor and Bioelectronics

Advances in electronic detection based on 1D nanomaterials provide the ability for label-free and real time, yet sensitive and selective, sensing biomolecules. The development of CNTs with unique electronic properties has been spotlighted for future solid-state nanoelectronics. Therefore, CNT-based molecular electronics have

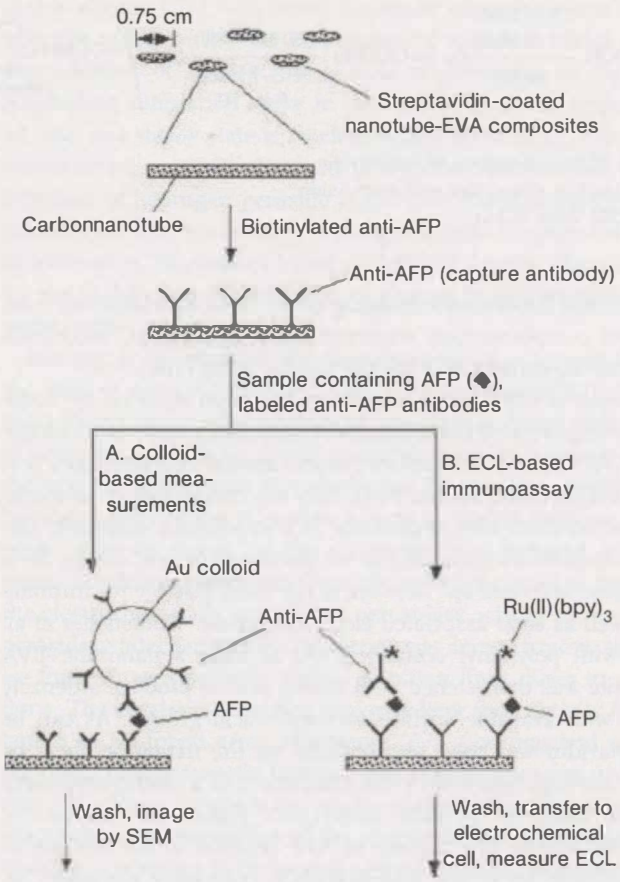

Fig. 3.14. Schematic of procedures for AFP assays based on the CNT-ECL sensor (not to scale). (Reprinted with permission from Ref. [105]. Copyright 2003 Wiley-VCH.)

received wide attention because of the semiconductor features of the nanotubes [109]. Among them, the study of CNT field-effect transistors (CNTFETs) is the core study to compare with the silicon-based transistors. The first CNTFETs were demonstrated by Tans et al. and Martel et al., respectively, in observing the CNTs' exploitable switching behavior [110, 133]. Since then, efforts have been made to improve the electrical characteristics of the CNTFETs. Presently, those explorable features of CNTFETs are the ballistic (scattering-free) and spin-conserving transport of electrons along the nanotubes, their ability to display metallic conducting as well as semiconducting behavior, and their access to the energy gap, which depends on the tube diameter and the rolling orientation of the tubes. CNTs also have extraordinarily high thermal conductivity. These unique properties make them behave similarly to conventional metal-oxide semiconductor field effect transistors

(MOSFETs) as well as differently, with a change from Schottky-barrier modulation at the contacts to bulk switching. These responding multiplicities, coupled with different CNT assembling approaches, offer various possible CNTFETs applications in biological diagnosis, e.g., proteins [5, 81] and cancer cell [111]. Chen and co-workers have demonstrated an exploration of SWCNT as a platform for investigating surface–protein and protein–protein binding and developing a highly specific electronic biosensor. They put SWCNT on a junction (drain and source) as shown in Fig. 3.15 [81]. The SWCNT was modified with polyethylene, which can reduce the non-specific interaction of proteins. A specific receptor was conjugated onto polyethylene-modified SWCNT. Therefore, the device can be highly specific in detecting proteins such as 10E3 m Ab (Fig. 3.4). The detection limit of this method was found to be about 340 ng mL^{-1} or 1.0 nM.

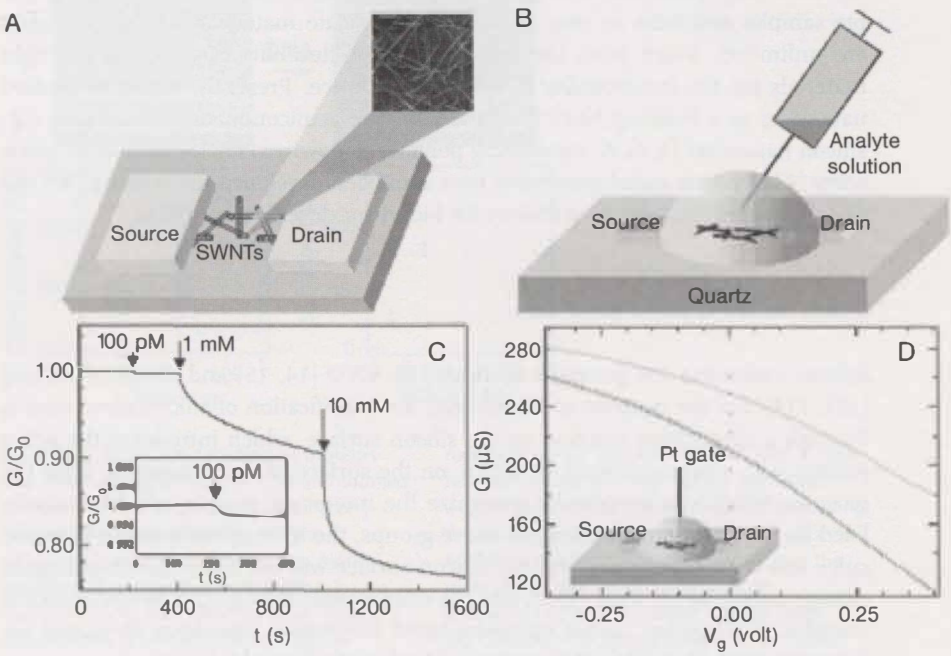

Fig. 3.15. Carbon nanotubes as electronic devices for sensing in aqueous solutions. (A) Schematic view of the electronic sensing device consisting of interconnected nanotubes bridging two metal electrode pads. An AFM image of a portion of the nanotube network (0.5 μm on a side) is shown. (B) Schematic setup for sensing in solution. (C) Conductance (G) evolution of a device for electronic monitoring of SA adsorption on nanotubes. The conductance is normalized by the initial conductance G_0. Inset: Sensitivity to a 100-pM protein solution. (D) Electrical conductance (G) vs. gate voltage (V_g) for a device in a 10-mM phosphate buffer solution. The gate voltage is applied through a Pt electrode immersed in the solution (inset). The upper (solid) and lower (broken) curves are the G–V_g characteristics for the device before and after SA binding, respectively. The shift in the two curves suggests a change in the charge environment of the nanotubes. (Reprinted with permission from Ref. [81]. © 2003 NAS).

3.3 Nanowires in Biosensor Development

Recently, nanowires have been explored as building blocks to fabricate nanoscale electronic devices through self-assembly – a typical bottom-up approach for biosensing [4, 6, 9]. The underlying mechanism for a nanowire biosensor is a field effect that is transduced using a field-effect transistor [4]. This "bottom-up" approach to bionanoelectronics has several attractive features. First, the nanowires are extremely sensitive for detection of biointeractions on their surface because of their high aspect ratio. Second, the electronically switchable properties of semiconducting nanowires provide a sensing modality, a direct and label-free electrical readout, which is exceptionally attractive. Third, the size of the nanowires can be readily tuned to sub-100 nm and smaller, which can lead to a high density of a device on a chip. Therefore, it is feasible for the miniaturized devices to detect multiple samples real time *in vivo*. Fourth, the candidate materials for the nanowires are unlimited, which gives the researcher great flexibility in selecting the right materials for the functionality of the desired device. Presently, the most studied nanowires as a building block for biosensing are semiconducting nanowires, e.g., silicon nanowires [4, 6, 9], conducting polymer nanowires [17, 18], and oxide nanowires [112]. Some metal nanowires have also been developed for sensing. We will focus on semiconducting nanowires for biosensor development here.

3.3.1 Silicon Nanowire-based Biosensors

Silicon nanowires are generally fabricated by CVD [14, 15] and template etching [113, 114]. For the purpose of biosensing, the modification of silicon nanowires is through a silanization reaction on the silicon surface, which introduces the active groups, e.g., amino, carboxyl, or biotin, on the surface of the nanowires. Then the receptor, which can specifically recognize the interested analyte, will be immobilized on the surface through those active groups, the interaction between biomolecules and their counterparts on the silicon surface will introduce the conductance change caused by the field effect, and the conductance change can be electronically transduced. Thus far, silicon nanowire-based biosensors have been developed for detection DNA [4, 8, 115, 116], proteins [4, 9], and viruses [6].

Lieber's group is pioneering the development of silicon nanowire-based biosensors [4, 8]. Biological macromolecules, such as proteins and nucleic acids, are typically charged in aqueous solutions and, as such, can be detected readily by nanowire sensors when appropriate receptors are linked to the nanowire active surface. Figure 3.16 shows the real time detection of proteins and DNA based on silicon nanowires. They modified silicon nanowires with biotin, which has a strong affinity to protein streptavidin on the oxide surface of nanowires [4]. When a solution of streptavidin is delivered to a nanowire sensor device modified with a biotin receptor, they found that the conductance of nanowires increases rapidly to a constant value, and this conductance value is maintained after the addition of pure buffer

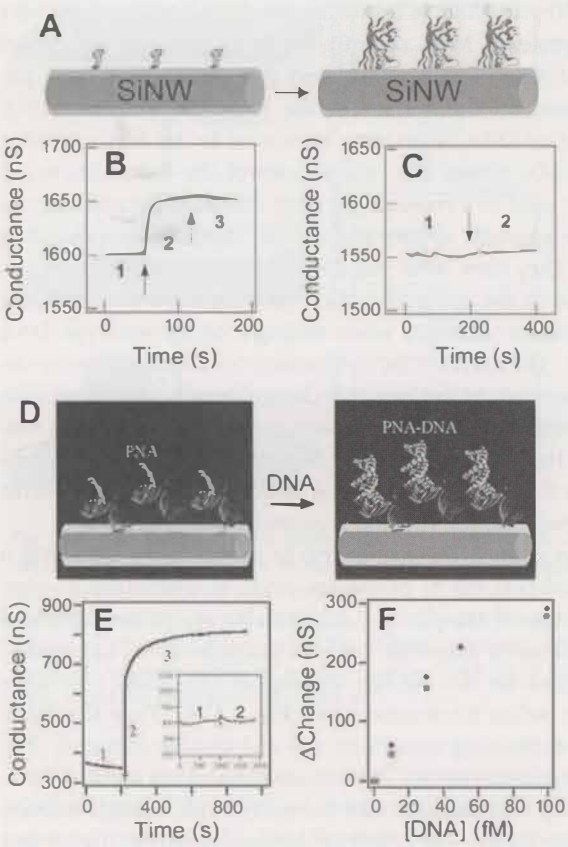

Fig. 3.16. Real-time detection of proteins and DNA. (A) Schematic of a biotin-modified Si nanowire and subsequent binding of streptavidin to the modified surface. (B) Conductance versus time for a biotin-modified Si nanowire, where Region 1 corresponds to the buffer solution, Region 2 corresponds to the addition of 250 nM streptavidin, and Region 3 corresponds to pure buffer solution. (C) Conductance versus time for an unmodified Si nanowire; Regions 1 and 2 are the same as in (B). (D) Schematic of a Si nanowire sensor surface modified with a PNA receptor before and after duplex formation with target DNA. (E) Si nanowire DNA sensing; the arrow corresponds to the addition of a 60-fM complementary DNA sample, and the inset shows the device conductance following addition of 100-fM mutant DNA. (F) Conductance versus DNA concentration; data points indicated by ■ and ● are obtained from two independent devices. (Reprinted with permission from Ref. [4], [8]. (A)–(C) 2001 © AAAS and (D)–(F) 2004 © ACS.)

(Fig. 3.16B). However, adding a streptavidin solution to unmodified silicon nanowires does not produce a change in conductance (Fig. 3.16C). The conductance change is caused by the specific interaction between biotin and streptavidin, and these results are further proved by an experiment in which blocking the streptavidin binding sites leads to an absence of response from biotin-modified silicon nanowires. They also studied the detection limit and found that the electrical detec-

tion could be carried out to 10 pM, which is below the detection level required for a number of disease marker proteins. More recently, a silicon nanowire field effect device has been investigated as a biosensor to detect the sequence of DNA [8]. First, a PNA was immobilized on the surface of the p-type Si nanowires (Fig. 3.16D). When a complementary DNA target was introduced to the device, the hybridization of DNA (Fig. 3.16D) caused the conductance of the nanowires to increase (Fig. 3.16E). PNA was used as a receptor for DNA detection because the uncharged PNA molecules have a greater affinity and stability than the corresponding DNA recognition sequence. They have used this device to detect the wild type versus the DF508 mutation site in the cystic fibrosis transmembrane receptor gene and showed that the conductance increases when adding a 60-fM wild-type DNA sample solution (Fig. 3.16E). The increase in conductance of the Si nanowire device is consistent with the increase in the negative charge density associated with the binding of negatively charged DNA at the surface, and moreover, careful control experiments show that the binding response is specific to the wild-type sequence. Further study shows that the direct electrical detection for DNA is possible down to at least the 10-fM level, and the method is reproducible (Fig. 3.16F).

The same group have also studied the use of the Si nanowire for detecting a single virus and demonstrated that the Si nanowires could be assembled to form arrays for multiplexed detection of samples [6]. Addressable arrays are fabricated by a process that uses a fluid-based assembly, such as microfluidic or Langmuir–Blodgett methods, to align and set the average spacing of nanowires over large areas for photolithography to define interconnections (Fig. 3.17A). They also fabricated a state-of-the art array containing more than 100 addressable elements (Fig. 3.17B). All the of the active nanowire sensor devices are confined to a central rectangular area on the device chip that overlaps with the microfluidic sample delivery channels, as illustrated in the figure. They further demonstrated the use of this nanowire array for detecting two types of virus at the same time. An antibody receptor that is specific either for influenza or for adenovirus was modified on p-type Si nanowires. Simultaneous conductance measurements were obtained when adenovirus, influenza, and a mixture of both viruses were delivered to the device. Other groups have also studied the use of silicon nanowires for DNA and protein analysis [115, 116].

3.3.2
Conducting Polymer Nanowire-based Biosensors

In recent years, conducting polymer-based nanostructured materials have been used extensively in resistive sensors [17]. Because of their promising properties, which include high surface areas, chemical specificities, tunable conductivities, material flexibilities, and easy processing, various methods have been developed to fabricate conducting polymer nanowires. For example, (a) polyaniline nanowires have been obtained through a facile synthesis [117] or by electrospinning methods [118]; (b) template-directed electrochemical processes have been employed to fabricate nanowire junctions that feature robust polymer electrode contacts [119]; and (c) mechanical stretching [120] and magnetic field-assisted assembly [121] pro-

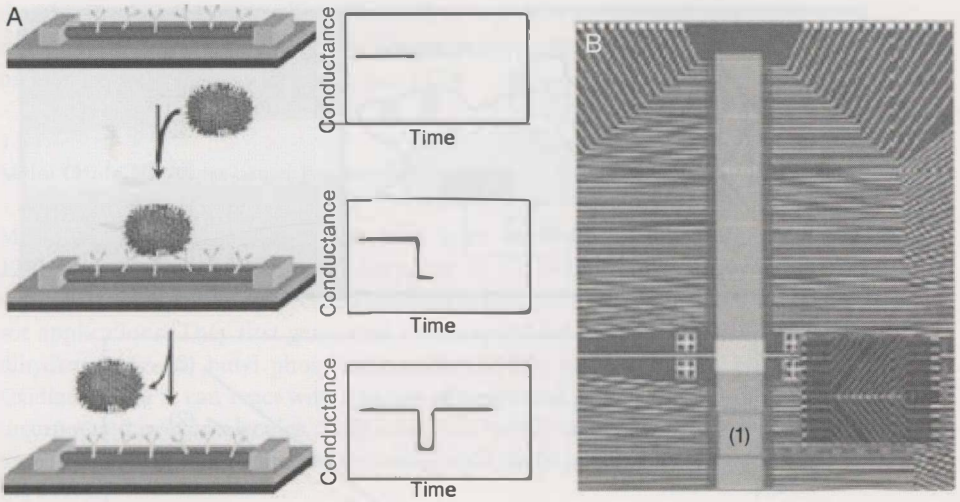

Fig. 3.17. (A) Schematic of a single virus binding and unbinding to the surface of a Si nanowire device modified with antibody receptors and the corresponding time-dependent change in conductance. (B) Optical image of the upper portion of a sensor device array, where the inset shows one row of individually addressable nanowire elements. The rectangle labeled (1) highlights the position of the microfluidic channel used to deliver samples and overlap the active elements. (Reprinted with permission from Ref. [6]. © 2004 NAS).

cesses have produced miniaturized polymer-electrode junctions. A templateless electrochemical assembly of conducting polymer nanowires has also been developed recently [17, 18]. The development of biosensors based on conducting polymer nanowires is still in its infancy. Some examples are introduced as follows.

Tao's group have demonstrated a glucose biosensor using conducting polymer/enzyme junctions and found that a unique feature can arise when shrinking a sensor to a nanometer [122]. Figure 3.18(A) shows the structure of the polymer/enzyme nanojunction sensor. The thickness of the polyaniline in the junction is 20–60 nm. The polyaniline/enzyme nanojunction was prepared by co-polymerization of monomer aniline and GOx in an aqueous solution. The signal transduction mechanism of the sensor is based on the changes in nanojunction conductance as a result of glucose oxidation induced change in the polymer redox state. Because of the small size of the nanojunction, they found that the response to glucose is fast and less than 1.0 s. However, the response time for glucose with a 10 μm gap is up to 10 min. The detection of limit for this method is at the μM level.

Myung's group has developed a facile technique for synthesizing conducting polymer nanowires by electrodeposition within channels between two electrodes on the surface of silicon wafers. They demonstrated that this technique can fabricate multiple individually addressable conducting polymer nanowires between two junctions. They also demonstrated the capability to create a scalable and high-density array by site-specific positioning of conducting polymer nanowires of the same and different composition on the same chip. Furthermore, the same group

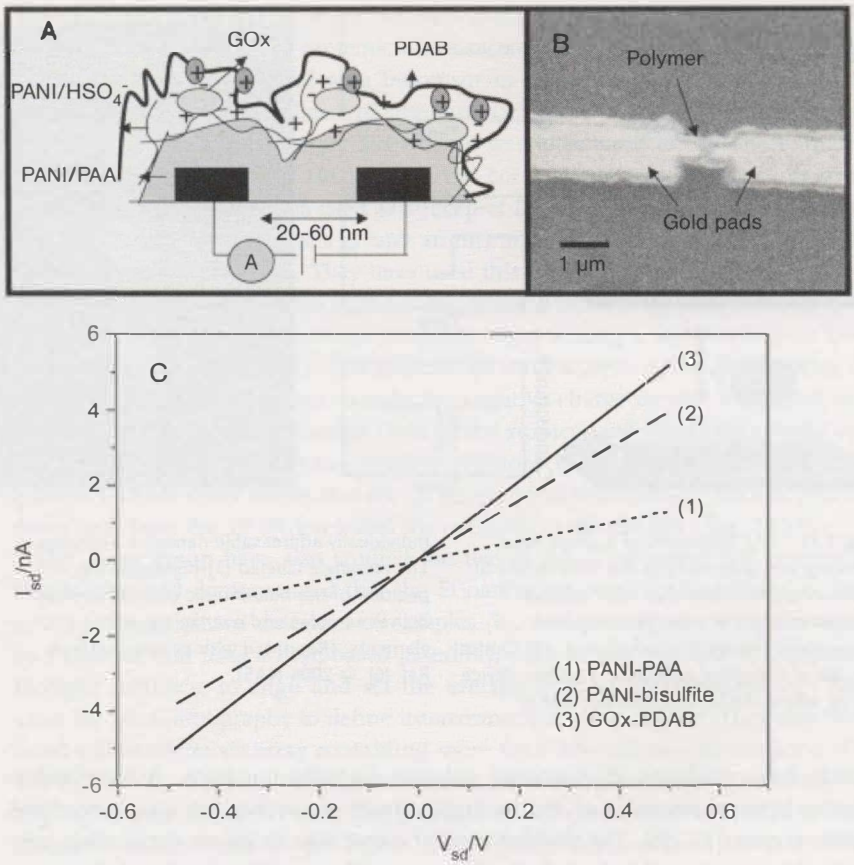

Fig. 3.18. (A) Structure of the polymer nanojunction sensor. (B) SEM image of PANI-PAA/PANI-bisulfite/GOx-PDAB films deposited on gold pads with gaps of 20–60 nm. (C) *I–V* curves obtained in air after each nanogap modification step: (1) polymerization of PANI-PAA carried out in 0.4 M aniline + 150 mg mL^{-1} PAA (MW: 2000) solution with 0.5 M Na_2SO_4 and 0.5 M H_2SO_4 by a potential sweep between −0.2 and 0.9 V vs. SCE during the first cycle and between −0.2 and 0.78 V vs. SCE during the following cycles at 0.05 V s^{-1}; (2) polymerization of PANI bisulfite in a 0.4 M aniline + 0.5 M $NaHSO_4$ solution acidified to pH 0 with H_2SO_4 by a single potential sweep from −0.2 to 0.9 V vs. SCE; (3) immobilization of GOx-PDAB by exposing the polymer nanojunction to 0.5 M Na_2SO_4 + 25 mM 1,2-diaminobenzene + 167 μM glucose oxidase in a pH 5 citric acid/Na_2HPO_4 (McIlvaine) buffer solution for 15 min, followed by electrodeposition of PDAB at +0.4 V vs. SCE for 4 min. (Reprinted with permission from Ref. [122]. © 2004 ACS).

reported bio-affinity sensing using biological functionalized conducting polymer nanowire. The device incorporated with polypyrrole nanowires made by the facile technique can be used for studying protein–protein interaction [123].

Wang et al. demonstrated template-free fabrication of polyaniline nanowire on electrode junctions by electrodeposition, and this method can be extended to syn-

thesize other conducting polymer nanowires, e.g., polypyrrole and poly(Edot). They systematically studied the electron transport properties of these conducting polymer nanowires with an electrolyte gate [124].

3.3.3
Metal Oxide Nanowire-based Biosensors

Metal oxide nanowires (MONWs) have been used to develop biosensors [112, 125]. They can work as a valid alternative to CNTs or Si NWs. Curreli and coworkers have reported a selective functionalization of In_2O_3 nanowires for biosensor applications. They first generated a self-assembled monolayer (SAM) of 4-(1,4-dihydroxybenzene) butyl phosphonic acid (HQ-PA) on the InO_2O_3 NW surface. Oxidized HQ-PA can react with a range of functional groups, which can be easily incorporated in biomolecules. They have successfully attached DNA on the In_2O_3, and this study opens an avenue for using such metal oxide nanowires for biosensing [112].

3.4
Nanocantilevers for Biosensors

Recently, microfabricated cantilevers have successfully been used for biosensors [126–132]. The adsorption of biomolecules on the surface will induce surface stress, which can be measured with micro/nanocantilevers. Adsorption of two proteins, immunoglobulin (IgG) and albumin (BSA), on a gold surface has been studied in a buffer solution in terms of surface stress measurements. Fritz and coworkers have reported the specific transduction, via surface stress changes, of DNA hybridization and receptor–ligand binding into a direct nanomechanic response of microfabricated cantilevers [126]. Cantilevers were fabricated in arrays and functionalized with a selection of biomolecules. The differential deflections of the cantilever were responses of individual cantilevers. Figure 3.19 illustrates the DNA hybridization on nanocantilevers in solution. First, a different sequence of DNA probe was modified on the surface of cantilevers (Fig. 3.19A), and then target DNA was injected. Only the cantilever that provides the matching sequence was found to have surface stress. It has been demonstrated that a single mismatch between 12-mer oligonucleotide is detectable. This method shows important advantages in that it does not require labeling, optical excitation, or external probes. In addition, the transduction process is repeatable and enables cyclic operation. At the same time, Hansen et al. have reported a cantilever-based optical deflection assay for discrimination of DNA single-nucleotide mismatches [127].

Furthermore, Wu and coworkers have extended this research to a real biological system, disease-related proteins. They reported that microcantilevers of different geometries have been used to detect two forms of prostate-specific antigens (PSAs) over a wide range of concentration range 0.2 ng mL^{-1} to 60 μg mL^{-1} in a background of human serum albumin and human plasminogen at 1.0 mg mL^{-1}

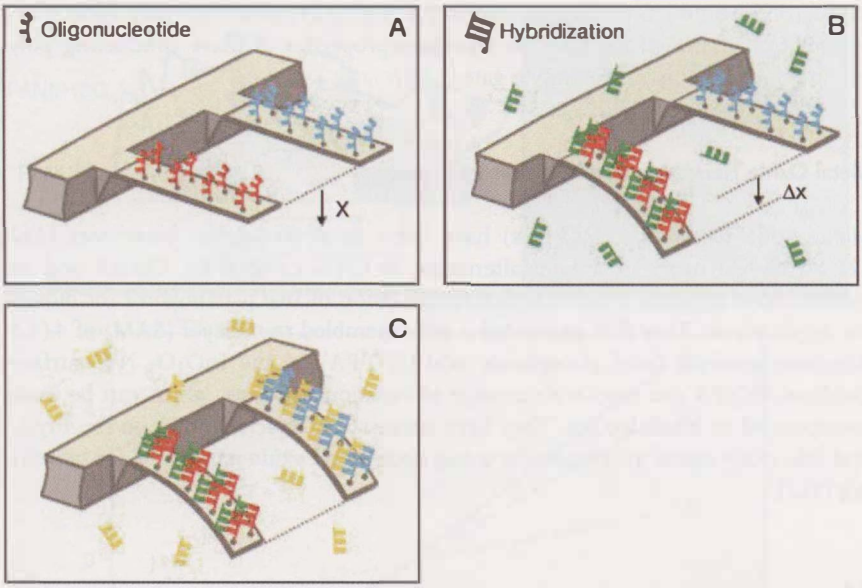

Fig. 3.19. Scheme illustrating the hybridization experiment. Each cantilever is functionalized on one side with a different oligonucleotide base sequence (red or blue). (A) The differential signal is set to zero. (B) After injection of the first complementary oligonucleotide (green), hybridization occurs on the cantilever that provides the matching sequence (red), increasing the differential signal Dx. (C) Injection of the second complementary oligonucleotide (yellow) causes the cantilever functionalized with the second oligonucleotide (blue) to bend.

[129]. This study makes this technique a clinically relevant diagnostic technique for prostate cancer.

3.5 Summary

One-dimensional nanomaterials, such as CNTs, semiconducting nanowires, and Si-based nanocantilevers have shown promise as new detection platforms that are equal or superior to many other sensing materials. This is mainly attributed to their unique electronic, mechanic, thermal, and chemical properties. The preparation, purification, and dispersion of single-walled and multiwalled nanotubes have, especially, been reviewed. Various sensor fabrication protocols based on those 1D nanomaterials have been discussed in detail. A typical application for DNA and proteins, including enzymes and antibodies, has been described, and the respective responding mechanisms have been addressed in this comprehensive review. Various 1D nanomaterial-based biosensors have found broad application from their

respective designs, including unmodified and surface-confined nanomaterials. Accordingly, biosensing based on amperometric amplification, field-effect transistors, signal-enhanced immunoassay, and non-enzymatic monitoring, and surface stress has been described for various biosensor designs. This research field is experiencing explosive growth, and new reports appear on a daily basis. We anticipate that the high orderly array design, combined with multiple biorecognition, will be the hotspot for the next stage of the 1D nanomaterial-based sensor studies.

Acknowledgments

The work performed at Pacific Northwest National Laboratory (PNNL) was supported by the Laboratory Directed Research and Development program, DOE-EMSP, SERDP (Project ID 1297), and NIH/1R01 ES010976-01A2. The authors' research described in this chapter was performed in part at the Environmental Molecular Sciences Laboratory, a national scientific user facility sponsored by the DOE Office of Biological and Environmental Research and located at PNNL. PNNL is operated for DOE by Battelle under Contract DE-AC05-76RL01830.

Glossary

Amperometry An electrochemical technique that measures electrical current at a fixed potential upon adding analyte or titrant into the measuring cell.

Biosensor Any probe designed to measure biological molecules' concentration or structures, monitor biological processes, or translate biochemical signals into quantifiable physical signals.

Carbon nanotube (CNT) A 1D fullerene with a cylindrical shape that consists of a seamless structure with hexagonal honeycomb lattices, being several nanometers in diameter and up to hundreds of microns long. CNTs can be divided into two major groups, i.e., single-wall carbon nanotubes (SWCNTs) and multiwall carbon nanotubes (MWCNTs). SWCNTs represent a single graphite sheet rolled flawlessly, demonstrating a tube diameter of 1 to 2 nm, whereas MWCNTs show concentric and closed graphite tubules with diameters ranging from 2 to 50 nm and an interlayer distance of approximately 0.34 nm.

Catalysis The acceleration of a chemical reaction by a catalyst.

Chemiluminescence A luminescence phenomenon produced by the direct transformation of chemical energy into light energy.

DNA Deoxyribonucleic acid. A naturally occurring polymer consisting of a phosphate backbone, sugar rings, and various bases. Usually it is found as single- or double-stranded deoxynucleotides.

Field effect transistor (FET) A semiconductor transistor with a region of donor material with two terminals designated as the "source" and the "drain," respectively, and an adjoining region of acceptor material in between, called the "gate."

The voltage between the gate and the substrate controls the current flow between the source and the drain by depleting the donor region of its charge carriers to a greater or lesser extent.

Enzyme electrode A type of biosensor that uses an enzyme-anchored electrode setup.

Hybridization The process of forming double stranded DNA molecules by combining two complementary single-stranded oligonucleotides.

Nafion A brand from a DuPont produced polymer that was synthesized by modifying a Teflon polymer. Like Teflon, Nafion is extremely chemically inert. However, unlike Teflon, Nafion is very ion-conductive because it contains sulfonic acid groups. These unique properties make Nafion useful in ion-exchange membranes, humidity sensors, fuel cells, etc.

Lithography A technique that creates chemical patterns on a metal or ceramic surface. It is currently used in making integrated electronic circuits, computer chips, etc.

Organophosphorus compounds Organic molecules that contain the element phosphorus. Organophosphorus (OP) compounds are very toxic and are thus widely used as pesticides and chemical-warfare agents (CWAs).

Polymer A macromolecule consisting of repeated chemical units.

Screen printing A traditional printing method that is used to print everything from T-shirts to coffee mugs and decals. It uses a squeegee to force ink through a stencil created on a mesh fabric onto some type of substrate such as a silk, metal, or stone. It is a mass production method. It has been used for fabricating sensors, such as single-use glucose strips.

Sol–gel technique A sol is a homogeneous dispersion of the solid particles (~100 to 1000 nm) in a liquid where only the Brownian motions suspend the particles. A gel is a state where both liquid and solid are dispersed in each other, which presents a solid network containing liquid components. The sol–gel technique is a low-temperature method using chemical precursors that can produce ceramics and glasses with better purity and homogeneity than high-temperature conventional processes. This technique currently has wide application in preparing electronic, optical, and electro-optic devices.

Abbreviations

1D	One-dimensional
AFM	Atomic-force microscopy
AFP	α-Fetoprotein
ALP	Alkaline phosphatase
BSA	Bovine serum albumin
CE	Capillary electrophoresis
CNT	Carbon nanotube
CNTFET	Carbon nanotube field-effect transistor
CVD	Catalytic vapor deposition

CWA	Chemical-warfare agent
DCC	Dicyclohexylcarbodiimide
DMF	*N*,*N*-Dimethylformamide
DNA	Deoxyribonucleic acid
DOE	U.S. Department of Energy
EAD	Electric arc discharge
ECL	Electrogenerated chemiluminescence
EVA	Poly(vinyl acetate)
FET	Field-effect transistor
GC	Gas chromatography
GOx	Glucose oxidase
HQ-PA	4-(1,4-Dihydroxybenzene) butyl phosphonic acid
HRP	Horseradish peroxidase
IgG	Immunoglobulin G
LA	Laser ablation
LC	Liquid chromatography
MONW	Metal oxide nanowire
MOSFET	Metal-oxide-semiconductor field effect transistor
MPDA	*m*-Phenylenediamine
mRNA	Message ribonucleic acid
MWCNT	Multiwall carbon nanotube
NADH	β-Nicotinamide adenine dinucleotide
NEA	Nanoelectrode array
PECVD	Plasma-enhanced chemical vapor deposition
PEG	Poly(ethylene glycol)
PNA	Peptide nucleic acid
PNNL	Pacific Northwest National Laboratory
Ppy	Polypyrrole
PSA	Prostate-specific antigen
RNA	Ribonucleic acid
SAM	Self-assembled monolayer
SpA	Staphylococcal protein A
SWCNT	Single-wall carbon nanotube
TEM	Transmission electron microscopy

References

1 Bachtold, A., Hadley, P., Nakanishi, T., Dekker, C. Logic circuits with carbon nanotube transistors, *Science* **2001**, 294, 1317–1320.

2 Rueckes, T., Kim, K., Joselevich, E., Tseng, G. Y., Cheung, C. L., Lieber, C. M. Carbon nanotube-based nonvolatile random access memory for molecular computing, *Science* **2000**, 289, 94–97.

3 Kong, J., Franklin, N. R., Zhou, C. W., Chapline, M. G., Peng, S., Cho, K. J., Dai, H. J. Nanotube molecular wires as chemical sensors, *Science* **2000**, 287, 622–625.

4 Cui, Y., Wei, Q. Q., Park, H. K., Lieber, C. M. Nanowire nanosensors for highly sensitive and selective detection of biological and chemical species, *Science* **2001**, 293, 1289–1292.

5 Star, A., Gabriel, J. C. P., Bradley, K., Gruner, G. Electronic detection of specific protein binding using nanotube FET devices, *Nano Lett.* **2003**, 3, 459–463.

6 Patolsky, F., Zheng, G. F., Hayden, O., Lakadamyali, M., Zhuang, X. W., Lieber, C. M. Electrical detection of single viruses, *Proc. Natl Acad. Sci. U.S.A.* **2004**, 101, 14 017–14 022.

7 So, H. M., Won, K., Kim, Y. H., Kim, B. K., Ryu, B. H., Na, P. S., Kim, H., Lee, J. O. Single-walled carbon nanotube biosensors using aptamers as molecular recognition elements, *J. Am Chem. Soc.* **2005**, 127, 11 906–11 907.

8 Hahm, J., Lieber, C. M. Direct ultrasensitive electrical detection of DNA and DNA sequence variations using nanowire nanosensors, *Nano Lett.* **2004**, 4, 51–54.

9 Wang, W. U., Chen, C., Lin, K. H., Fang, Y., Lieber, C. M. Label-free detection of small-molecule-protein interactions by using nanowire nanosensors, *Proc. Natl Acad. Sci. U.S.A.* **2005**, 102, 3208–3212.

10 Xia, Y. N., Yang, P. D., Sun, Y. G., Wu, Y. Y., Mayers, B., Gates, B., Yin, Y. D., Kim, F., Yan, Y. Q. One-dimensional nanostructures: Synthesis, characterization, and applications, *Adv. Mater.* **2003**, 5, 353–389.

11 Law, M., Goldberger, J., Yang, P. D. Semiconductor nanowires and nanotubes, *Ann. Rev. Mater. Res.* **2004**, 34, 83–122.

12 Nikolaev, P., Bronikovski, M. J., Bradley, K., Rohmund, F., Colbert, D. T., Smith, K. A., Smalley, R. E. Gas-phase catalytic growth of single-walled carbon nanotubes from carbon monoxide, *Chem. Phys. Lett.* **1999**, 313, 91–97.

13 Amelinckx, S., Zhang, B., Bernaerts, J., Zhang, X. F., Ivanov, V., Nagy, J. B. A formation mechanism for catalytically grown helix-shaped graphite nanotubes, *Science*, **1996**, 265, 635–639.

14 Niu, J. J., Sha, H., Wang, Y. W., Ma, X. Y., Yang, D. R. Crystallization and disappearance of defects of the annealed silicon nanowires, *Microelectron. Eng.* **2003**, 66, 65–69.

15 Wu, Y., Fan, R., Yang, P. D. Block-by-block growth of single-crystalline Si/SiGe superlattice nanowires, *Nano Lett.* **2002**, 2, 83–86.

16 Cheng, S. W., Cheung, H. F. Role of electric field on formation of silicon nanowires, *J. Appl. Phys.* **2003**, 94, 1190–1194.

17 Wang, J., Chan, S., Carlson, R. R., Luo, Y., Ge, G. L., Ries, R. S., Heath, J. R., Tseng, H. R. Electrochemically fabricated polyaniline nanoframework electrode junctions that function as resistive sensors, *Nano Lett.* **2004**, 4, 1693–1697.

18 Liang, L., Liu, J., Windisch, C. F., Exarhos, G. J., Lin, Y. H. Direct assembly of large arrays of oriented conducting polymer nanowires, *Angew. Chem. Int. Ed.* **2002**, 41, 3665–3668.

19 Wang, J., Liu, G., Jan, M. Ultrasensitive electrical biosensing of proteins and DNA: Carbon-nanotube derived amplification of the recognition and transduction events, *J. Am. Chem. Soc.* **2004**, 126, 3010.

20 O'Connor, M., Kim, S. N., Kiliard, A. J., Forster, R. J., Smyth, M. R. Papadimitrakopoulos, F., Rusling, J. F. Mediated amperometric immunosensing using single walled carbon nanotube forests, *Analyst* **2004**, 129, 1176–1180.

21 Xu, J. M. Highly ordered carbon nanotube arrays and IR detection, *Infra. Phys. Tech.* **2001**, 42, 485–491.

22 Fritz, J., Baller, M. K., Lang, H. P., Strunz, T., Meyer, E., Guntherodt, H. J., Delamarche, E., Gerber, C., Gimzewski, J. K. Stress at the solid-liquid interface of self-assembled monolayers on gold investigated with a nanomechanical sensor, *Langmuir* **2000**, 16, 9694–9696.

23 Wang, J. X., Li, M. X., Shi, Z. J., Li, N. Q., Gu, Z. N. Direct electro-

chemistry of cytochrome c at a glassy carbon electrode modified with single-wall carbon nanotubes, *Anal. Chem.* **2002**, 74, 1993–1997.

24 Wang, J. Nanomaterial-based electrochemical biosensors, *Analyst* **2005**, 130, 421–426.

25 Kohli, P., Wirtz, M., Martin, C. R. Nanotube membrane based biosensors, *Electroanalysis* **2004**, 16, 9–18.

26 Iijima, S. N. Helical microtubules of graphitic carbon, *Nature*, **1991**, 354, 56–58.

27 Kroto, H. W., Heath, J. R., O'Brien, S. C., Curl, R. F., Smalley, R. E. C-60 – buckminsterfullerene, *Nature*, **1985**, 318, 162–163.

28 Ajayan, P. M. Carbon naonotube from carbon, *Chem. Rev.* **1999**, 99, 1787–1799.

29 Harris, P. J. F. *Carbon Nanotubes and Related Structures*, Cambridge University Press, Cambridge, UK, **1999**.

30 Thostenson, E. T., Ren, Z. F., Chou, T. W. C. Advances in the science and technology of carbon nanotubes and their composites: A review, *Compos. Sci. Technol.* **2001**, 61, 1899–1912.

31 Popov, V. N. Carbon nanotubes: Properties and application, *Mater. Sci. Eng. R: Rep.*, **2004**, 43, 61–102.

32 Kohli, P., Martin, C. R. The emerging field of nanotube biotechnology, *Nat. Rev. Drug Discov.* **2003**, 2, 29–37.

33 Sinnott, S. B. Chemical functionalization of carbon nanotubes, *J. Nanosci. Nanotechnol.* **2002**, 2, 113–123.

34 Baughman, R. H., Zakhidov, A. A., de Heer, W. A. Carbon nanotubes – the route toward applications, *Science*, **2002**, 297, 787–792.

35 Ouyang, M., Huang, J., Lieber, C. M. Fundamental electronic properties and applications of single-walled carbon nanotubes, *Acc. Chem. Res.* **2002**, 35, 1018–1025.

36 Britto, P. J., Sunthanam, K. S. V., Ayajan, P. M. Carbon nanotube electrode for oxidation of dopamine, *Bioelectrochem. Bioenerg.* **1996**, 41, 121–125.

37 Besteman, K., Lee, J., Wiertz, F. G. M., Heering, H. A., Dekker, C. Enzyme-coated carbon nanotubes as single-molecule biosensors, *Nano Lett.* **2003**, 3, 727–730.

38 Salimi, A., Banks, C. E., Compton, R. G. Abrasive immobilization of carbon nanotubes on a basal plane pyrolytic graphite electrode: Application to the detection of epinephrine, *Analyst*, **2004**, 129, 225–228.

39 Wang, J., Musameh, M. Carbon nanotube screen-printed electrochemical sensors, *Analyst*, **2004**, 129, 1–2.

40 Pedano, M. L., Rivas, G. A. Adsorption and electrooxidation of nucleic acids at carbon nanotubes paste electrodes, *Electrochem. Commun.* **2004**, 6, 10–16.

41 Lin, Y., Taylor, S., Li, H. P., Fernando, K. A. S., Qu, L. W., Wang, W., Gu, L. R., Zhou, B., Sun, Y. P. Advances toward bioapplications of carbon nanotubes, *J. Mater. Chem.* **2004**, 14, 527–541.

42 Martin, C. R., Kohli, P. The emerging field of nanotube biotechnology, *Nat. Rev. Drug Discov.*, **2003**, 2, 29–37.

43 Li, N., Wang, J., Li, M. *Rev. Anal. Chem.* **2003**, 22, 19.

44 Odom, T. W., Huang, J. L., Lieber, C. M. Single-walled carbon nanotubes – From fundamental studies to new device concepts, *Ann. N. Y. Acad. Sci.* **2002**, 960, 203–215.

45 Thess, A., Lee, R., Nikolaev, P., Dai, H., Petit, H., Robert, J., Xu, D., Lee, Y. H., Kim, S. G., Rinzler, A. G., Colbert, D. T., Scuseria, G., Tomanek, D., Fisher, J. E., Smalley, R. E. Crystalline ropes of metallic carbon nanotubes, *Science*, **1996**, 273, 483–487.

46 Xie, S., Li, W., An, Z., Chang, B., Sun, L. *Mater. Sci. Eng. A*, **2000**, 286, 11.

47 Yacaman, M. J., Yoshida, M. M., Rendon, L., Santiesteban, J. G. Catalytic growth of carbon microtubules with fullerene structure, *Appl. Phys. Lett.*, **1993**, 62, 202.

48 Ivanov, V., Nagy, J. B., Lambin, P., Lucas, A., Zhang, X. B., Zhang,

X. F., Bernaerts, D., Van Tendeloo, G., Amelinckx, S., Van Landuyt, J. The study of carbon nanotubules produced by catalytic method, *Chem. Phys. Lett.* 1994, 223, 329–335.

49 Yudasaka, M., Kituchi, R., Matsui, T., Ohki, Y., Yoshimura, S. Specific conditions for Ni catalyzed carbon nanotube growth by chemical vapor deposition, *Appl. Phys. Lett.* 1995, 67, 2477–2479.

50 Iijima, S., Ichihashi, T. Single-shell carbon nanotubes of 1-nm diameter, *Nature*, 1993, 363, 603–605.

51 Kong, J., Soh, H., Cassell, A. M., Quate, C. F., Dai, H. J. Synthesis of individual single-walled carbon nanotubes on patterned silicon wafers, *Nature* 1998, 395, 878–881.

52 Colomer, J. F., Bister, G., Willems, I., Konya, Z., Fonseca, A., Van Tendeloo, G., Nagy, J. B. Synthesis of single-wall carbon nanotubes by catalytic decomposition of hydrocarbons, *Chem. Commun.* 1998, 1343–1344.

53 Shelimov, K. B., Esenaliev, R. O., Rinzler, A. G., Huffman, C. B., Smalley, R. E. Purification of single-wall carbon nanotubes by ultrasonically assisted filtration, *Chem. Phys. Lett.* 1998, 282, 429–434.

54 Tohji, K., Goto, T., Takahashi, H., Shinoda, Y., Shimizu, N., Jeyadevan, B., Saito, I., Miasuoka, Y., Kasuya, A., Ohsuna, T., Hiraga, K., Nashina, Y. Purifying single-walled nanotubes, Nature 1996, 383, 679.

55 Zhou, O., Gao, B., Bower, D., Fleming, L., Shimoda, H. Structure and electrochemical properties of carbon nanotube intercalation compounds, *Mol. Cryst. Liq. Cryst.* 2000, 340, 541.

56 Liu, J., Rinzler, A. G., Dai, H., Hafner, J. H., Bradley, R. K., Boul, P. J., Lu, A., Iverson, T., Shelimov, K., Huffman, C. B., Rodriguez-Macias, F., Shon, Y. S., Lee, T. R., Colbert, D. T., Smalley, R. E. Fullerene pipes, *Science* 1998, 280, 1253–1256.

57 Kovtyukhova, N. I., Mallouk, T. E., Pan, L., Dickey, E. C. Individual single-walled nanotubes and hydrogels made by oxidative exfoliation of carbon nanotube ropes, *J. Am. Chem. Soc.* 2003, 125, 9761–9769.

58 Shaffer, M. S. P., Windle, A. H. Analogies between polymer solutions and carbon nanotube dispersions, *Macromolecules* 1999, 32, 6864–4866.

59 Star, A., Stoddart, J. F., Steuerman, D., Diehl, M., Boukai, A., Wong, E. W., Yang, X., Chung, S., Choi, H., Heath, J. R. Preparation and properties of polymer-wrapped single-walled carbon nanotubes, *Angew. Chem. Int. Ed.* 2001, 40, 1721–1275.

60 Riggs, J. E., Guo, Z. X., Carroll, D. L., Sun, Y. P. Strong luminescence of solubilized carbon nanotubes, *J. Am. Chem. Soc.* 2000, 122, 5879–5880.

61 Wang, J., Musameh, M., Lin, Y. Solubilization of carbon nanotubes by Nafion toward the preparation of amperometric biosensors, *J. Am. Chem. Soc.* 2003, 125, 2408–2409.

62 Star, A., Han, T., Joshi, V., Stetter, J. R. Sensing with Nafion coated carbon nanotube field-effect transistors, *Electroanalysis* 2004, 16, 108–112.

63 Wang, J., Liu, G., Jan, M. R. Ultrasensitive electrical biosensing of proteins and DNA: Carbon-nanotube derived amplification of the recognition and transduction events, *J. Am. Chem. Soc.* 2004, 126, 3010–3011.

64 Wang, J., Chen, G., Chatrathi, M. P., Musameh, M. Capillary electrophoresis microchip with a carbon nanotube-modified electrochemical detector, *Anal. Chem.* 2004, 76, 298–302.

65 Liu, Z., Shen, Z., Zhu, T., Hou, S., Ying, L., Shi, Z., Gu, Z. Organizing single-walled carbon nanotubes on gold using a wet chemical self-assembling technique, *Langmuir* 2003, 16, 3569–3573.

66 Gooding, J. J., Wibowo, R., Liu, J., Yang, W., Losic, D., Orbons, S., Mearns, F. J., Shapter, J. G., Hibbert, D. B. Protein electrochemistry using aligned carbon nanotube

arrays, *J. Am. Chem. Soc.* 2003, 125, 9006–9007.

67 Yu, X., Chattopadhyay, D., Galeska, I., Papadimitrakopoulos, F., Rusling, J. F. Peroxidase activity of enzymes bound to the ends of single-wall carbon nanotube forest electrodes, *Electrochem. Commun.* 2003, 5, 408–411.

68 Kim, B., Sigmund, W. M. Self-alignment of shortened multiwall carbon nanotubes on polyelectrolyte layers, *Langmuir* 2003, 19, 4848–4851.

69 Azamian, B. R., Davis, J. J., Coleman, K. S., Bagshaw, C. B. B., Green, M. L. J. Bioelectrochemical single-walled carbon nanotubes, *J. Am. Chem. Soc.* 2002, 124, 12 664–12 665.

70 Davis, J. J., Coleman, K. S., Azamian, B. R., Bagshaw, C. B., Green, M. L. H. Mical and biochemical sensing with modified single walled carbon nanotubes, *Chem. Eur. J.* 2003, 9, 3732–3739.

71 Azamian, B. R., Coleman, K. S., Davis, J. J., Hanson, N., Green, M. L. J. Directly observed covalent coupling of quantum dots to single-wall carbon nanotubes, *Chem. Commun.* 2002, 366.

72 Ajayan, P. M., Stephan, O., Colliex, C., Trauth, D. Aligned carbon nanotube arrays formed by cutting a polymer resin-nanotube composite, *Science* 1994, 265, 1212–1214.

73 Gao, M., Dai, L., Wallace, G. G. Biosensors based on aligned carbon nanotubes coated with inherently conducting polymers, *Electroanalysis* 2003, 15, 1089–1094.

74 Xu, Y., Jiang, Y., Cai, H., He, P., Fang, Y. Electrochemical impedance detection of DNA hybridization based on the formation of M-DNA on polypyrrole/carbon nanotube modified electrode, *Anal. Chim. Acta* 2004, 516, 19–27.

75 Gavalas, V. G., Law, S. A., Christopher, B. J., Andrews, R., Bachas, Carbon, L. G. Nanotube aqueous sol-gel composites: Enzyme-friendly platforms for the development of stable biosensors, *Anal. Biochem.* 2004, 329, 247–252.

76 Wang, J., Musameh, M. Carbon nanotube/Teflon composite electrochemical sensors and biosensors, *Anal. Chem.* 2003, 75, 2075–2079.

77 Hrapovic, S., Liu, Y., Male, K. B., Luong, J. H. Electrochemical biosensing platforms using platinum nanoparticles and carbon nanotubes, *Anal. Chem.* 2004, 76, 1083–1088.

78 Tang, H., Chen, J., Yao, S., Nie, L., Deng, G., Kuang, Y. Carbon nanotube aqueous sol-gel composites: Enzyme-friendly platforms for the development of stable biosensors, *Anal. Biochem.* 2004, 331, 97–252.

79 Wang, J., Liu, G., Jan, M. R., Zhu, Q. Electrochemical detection of DNA hybridization based on carbon-nanotubes loaded with CdS tags, *Electrochem. Commun.* 2003, 5, 1000–1004.

80 Chen, R. J., Zhang, Y., Wang, D., Dai, H. Noncovalent sidewall functionalization of single-walled carbon nanotubes for protein immobilization, *J. Am. Chem. Soc.* 2001, 123, 3838–3839.

81 Chen, R. J., Bangsaruntip, S., Drouvalakis, K. A., Kam, N., Shim, M., Li, Y., Kim, W., Utz, P. J., Dai, H. Noncovalent functionalization of carbon nanotubes for highly specific electronic biosensors, *Proc. Natl. Acad. Sci. U.S.A.* 2003, 100, 4984–4989.

82 Besteman, K., Lee, J.-O., Wiertz, F. G. M., Heering, H. A., Dekker, C. Enzyme-coated carbon nanotubes as single-molecule biosensors, *Nano Lett.* 2003, 3, 727–730.

83 Baker, S. E., Cai, W., Lasseter, T. L., Weidkamp, K. P., Hamers, R. J. Covalently bonded adducts of deoxyribonucleic acid (DNA) oligonucleotides with single-wall carbon nanotubes: Synthesis and hybridization, *Nano Lett.*, 2002, 2, 1413–1417.

84 Hazani, M., Naaman, R., Hennrich, F., Kappes, M. M. Confocal fluorescence imaging of DNA-functionalized carbon nanotubes, *Nano Lett.*, 2003, 3, 153–155.

85 Williams, K. A., Veenhuizen, P. T. M., de la Torre, B. G., Eritja,

R., Dekker, C. Nanotechnology: Carbon nanotubes with DNA recognition, *Nature* **2002**, 420, 761.

86 Melle-Franco, M., Marcaccio, M., Paolucci, D., Paolucci, F., Georgakilas, V. D., Guldi, M., Prato, M., Zerbetto, F. Cyclic voltammetry and bulk electronic properties of soluble carbon nanotubes, *J. Am. Chem. Soc.* **2004**, 126, 1646–1647.

87 Zhao, Y., Zhang, W., Chen, H., Luo, Q. Electrocatalytic oxidation of cysteine at carbon nanotube powder microelectrode and its detection, *Sen. Actuators, B: Chem.* **2003**, 92, 279–285.

88 Wang, Z., Liu, J., Liang, Q., Wang, Y., Luo, G. Carbon nanotube-modified electrodes for the simultaneous determination of dopamine and ascorbic acid, *Analyst* **2002**, 127, 653.

89 Wang, Z., Wang, Y., Luo, G. A selective voltammetric method for uric acid detection at β-cyclodextrin modified electrode incorporating carbon nanotubes, *Analyst*, **2002**, 127, 1353.

90 Wu, K., Fei, J., Hu, S. Simultaneous determination of dopamine and serotonin on a glassy carbon electrode coated with a film of carbon nanotubes, *Anal. Biochem.* **2003**, 318, 100–106.

91 Musameh, M., Wang, J., Merkoci, A., Lin, Y. Low-potential stable NADH detection at carbon-nanotube-modified glassy carbon electrodes, *Electrochem. Commun.* **2002**, 4, 743–746.

92 Ye, J., Wen, Y., Zhang, W., Gan, L. M., Xu, G., Sheu, F. Nonenzymatic glucose detection using multi-walled carbon nanotube electrodes, *Electrochem. Commun.* **2004**, 6, 66–70.

93 Li, J., Ng, H. T., Cassell, A., Fan, W., Chen, H., Ye, Q., Koehne, J., Han, J., Meyyappan, M. Carbon nanotube nanoelectrode array for ultrasensitive DNA detection *Nano Lett.* **2003**, 3, 597–602.

94 Boussaad, S., Tao, N. J., Zhang, R., Hopson, T., Nagahara, L. A. *In situ* detection of cytochrome c adsorption with single walled carbon nanotube device, *Chem. Commun.* **2003**, 1502.

95 Xin, H., Woolley, A. T. DNA-templated nanotube localization, *J. Am. Chem. Soc.* **2003**, 125, 8710–8711.

96 Reyes, D. R., Iossifidis, D., Auroux, P. A., Manz, A. Micro total analysis systems. 1. Introduction, theory, and technology, *Anal. Chem.* **2002**, 74, 2623–2636.

97 Yamamoto, K., Shi, G., Zhou, T., Xu, F., Xu, J., Kato, T., Jin, J. Y., Jin, L. Study of carbon nanotubes–HRP modified electrode and its application for novel on-line biosensors, *Analyst*, **2003**, 128, 249.

98 Ghosh, S., Sood, A. K., Kumar, N. Carbon nanotube flow sensors, *Science*, **2003**, 299, 1042–1044.

99 Lin, Y., Lu, F., Wang, J. Disposable carbon nanotube modified screen-printed biosensor for amperometric detection of organophosphorus pesticides and nerve agents, *Electroanalysis* **2004**, 16, 145–149.

100 Morf, W. E., De Rooij, N. F. Performance of amperometric sensors based on multiple microelectrode arrays, *Sens. Actuators, B-Chem.*, **1997**, 44, 538–541.

101 Tu, Y., Lin, Y., Ren, Z. F. Nanoelectrode arrays based on low site density aligned carbon nanotubes, *Nano Lett.* **2003**, 3, 107–109.

102 Ng, H. T., Fang, A., Li, J., Li, S. F. Flexible Carbon nanotubes membrane sensory system – A generic platform, *J. Nanosci. Nanotechnol.* **2001**, 1, 375–379.

103 Lin, Y., Lu, F., Tu, Y., Ren, Z. Glucose biosensors based on carbon nanotube nanoelectrode ensembles, *Nano Lett.* **2004**, 4, 191–195.

104 He, P., Dai, L. Aligned carbon nanotube–DNA electrochemical sensors, *Chem. Commun.* **2004**, 3, 348.

105 Wohlstadter, J. N., Wilbur, J. L., Sigal, G. B., Biebuyck, H. A., Billiadeau, M. A., Dong, L., Fischer, A. B., Gudibande, S. R., Jameison, S. H., Kenten, J. H., Leginus, J., Leiand, J. K., Massey, R. J., Wohlstadter, S. J. Carbon nanotube-based biosensor, *Adv. Mater.* **2003**, 15, 1184–1187.

106 Guo, Z., Dong, S. Electrogenerated chemiluminescence from $Ru(Bpy)_3^{2+}$ ion-exchanged in carbon nanotube/perfluorosulfonated ionomer composite films, *Anal. Chem.* **2004**, 76, 2683–2688.

107 Hazani, M., Naaman, R., Hennrich, F., Kappes, M. M. Confocal fluorescence imaging of DNA-functionalized carbon nanotubes, *Nano Lett.* **2003**, 3, 153–155.

108 Baker, S. E., Cai, W., Lasseter, T. L., Weidkamp, K. P., Hamers, R. J. Covalently bonded adducts of deoxyribonucleic acid (DNA) oligonucleotides with single-wall carbon nanotubes: Synthesis and hybridization, *Nano Lett.* **2002**, 2, 1413–1417.

109 Dai, H. Carbon nanotubes: Synthesis, integration, and properties, *Acc. Chem. Res.* **2002**, 35, 1035–1044.

110 Tans, S. J., Verschueren, A. R. M., Dekker, C. *Nature*, **1998**, 393, 49.

111 Kam, N. W. S., O'Connell, M., Wisdom, J. A., Dai, H. J. Carbon nanotubes as multifunctional biological transporters and near-infrared agents for selective cancer cell destruction, *Proc. Natl. Acad. Soc. U.S.A.* **2005**, 102, 11 600–11 605.

112 Curreli, M., Li, C., Sun, Y. H., Lei, B., Gundersen, M. A., Thompson, M. E., Zhou, C. W. Selective functionalization of In2O3 nanowire mat devices for biosensing applications, *J. Am. Chem. Soc.* **2005**, 127, 6922–6923.

113 Melosh, N., Boukai, A., Diana, F., Gerardot, B., Badolato, A., Petroff, P., Heath, J. R. Ultrahigh density nanowire lattices and circuits, *Science*, **2003**, 300, 112.

114 Juhasz, R., Elfstrom, N., Linnros, J. Controlled fabrication of silicon nanowires by electron beam lithography and electrochemical size reduction, *Nano Lett.* **2005**, 5, 275–280.

115 Li, Z., Chen, Y., Li, X., Kamins, T. I., Nauka, K., Williams, R. S. Sequence-specific label-free DNA sensors based on silicon nanowires, *Nano Lett.* **2004**, 4, 245–247.

116 Li, Z., Rajendran, B., Kamins, T. I., Li, X., Chen, Y., Williams, R. S. Silicon nanowires for sequence-specific DNA sensing: Device fabrication and simulation, *Appl. Phys. A-Mater. Sci. Proc.* **2005**, 80, 1257–1263.

117 Huang, J. X., Virji, S., Weiller, B. H., Kaner, R. B. Polyaniline nanofibers: Facile synthesis and chemical sensors, *J. Am. Chem. Soc.* **2003**, 125, 314–315.

118 Kameoka, J., Verbridge, S. S., Liu, H. Q., Czaplewski, D. A., Craighead, H. G. Fabrication of suspended silica glass nanofibers from polymeric materials using a scanned electrospinning source, *Nano Lett.* **2004**, 4, 2105–2108.

119 Ramanathan, K., Bangar, M. A., Yun, M. H., Chen, W. F., Mulchandani, A., Myung, N. V. Individually addressable conducting polymer nanowires array, *Nano Lett.* **2004**, 4, 1237–1239.

120 He, H. X., Li, C. Z., Tao, N. J. Conductance of polymer nanowires fabricated by a combined electrodeposition and mechanical break junction method, *Appl. Phys. Lett.* **2001**, 78, 811–813.

121 Zhang, H., Boussaad, S., Ly, N., Tao, N. J. Magnetic field-assisted assembly of metal/polymer/metal junction sensor, *Appl. Phys. Lett.*, **2004**, 84, 133–135.

122 Forzani, E. S., Zhang, H. Q., Nagahara, L. A., Amlani, I., Tsui, R., Tao, N. J. A conducting polymer nanojunction sensor for glucose detection, *Nano Lett.* **2004**, 4, 1785–1788.

123 Ramanathan, K., Bangar, M. A., Yun, M., Chen, W., Myung, N. V. Mulchandani, A. Bioaffinity sensing using biologically functionalized conducting-polymer nanowire, *J. Am. Chem. Soc.* **2005**, 127, 496–497.

124 Aiam, M. M., Wang, J., Guo, Y. Y., Lee, S. P., Tseng, H. R. Electrolyte-gated transistors based on conducting polymer nanowire junction arrays, *J. Phys. Chem. B* **2005**, 109, 12 777–12 784.

125 Zhang, D. H., Liu, Z. Q., Li, C., Tang, T., Liu, X. L., Han, S., Lei, B., Zhou, C. W. Detection of NO2 down to ppb levels using individual and multiple In2O3 nanowire devices, *Nano Lett.* **2004**, 4, 1919–1924.

126 Fritz, J., Baller, M. K., Lang, H. P., Rothuizen, H., Vettiger, P., Meyer, E., Guntherodt, H. J., Gerber, C., Gimzewski, J. K. Translating biomolecular recognition into nanomechanics, *Science* **2000**, 288, 316–318.

127 Hansen, K. M., Ji, H. F., Wu, G. H., Datar, R., Cote, R., Majumdar, A., Thundat, T. Cantilever-based optical deflection assay for discrimination of DNA single-nucleotide mismatches, *Anal. Chem.* **2001**, 73, 1567–1571.

128 Stevenson, K. A., Mehta, A., Sachenko, P., Hansen, K. M., Thundat, T. Nanomechanical effect of enzymatic manipulation of DNA on microcantilever surfaces, *Langmuir* **2002**, 18, 8732–8736.

129 Wu, G. H., Datar, R. H., Hansen, K. M., Thundat, T., Cote, R. J., Majumdar, A. Bioassay of prostate-specific antigen (PSA) using microcantilevers, *Nat. Biotechnol.* **2001**, 19, 856–860.

130 Tian, F., Hansen, K. M., Ferrell, T. L., Thundat, T. Dynamic microcantilever sensors for discerning biomolecular interactions, *Anal. Chem.* **2005**, 77, 1601–1606.

131 Su, M., Li, S. U., Dravid, V. P. Microcantilever resonance-based DNA detection with nanoparticle probes, *Appl. Phys. Lett.* **2003**, 82, 3562–3564.

132 Chen, H., Han, J., Li, J., Meyyappan, M. Microelectronic DNA assay for the detection of BRCA1 gene mutations, *Biomed. Microdev.* **2004**, 6, 55–60.

133 Martel, R., Schmidt, T., Shea, H. R., Hertel, T., Avouris, PH. Single- and multiwall carbon nanotube field-effect transistors, *Appl. Phys. Lett.* **1998**, 73, 2447–2449.